Systematic errors in weak lensing cosmology

ZHANG Pengjie
Department of Astronomy & Tsung-Dao Lee Institute
Shanghai Jiao Tong University

April 16, 2020
Department of Astronomy, Tsinghua University

Outline

- Weak lensing cosmology
- Systematic errors in weak lensing cosmology
  - The intrinsic alignment
  - Self-calibrating the intrinsic alignment

Gravitational lensing

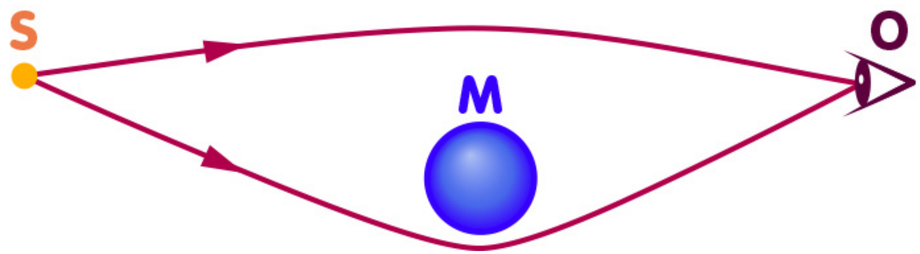

1912 note. Also, 1915 letter to a friend.

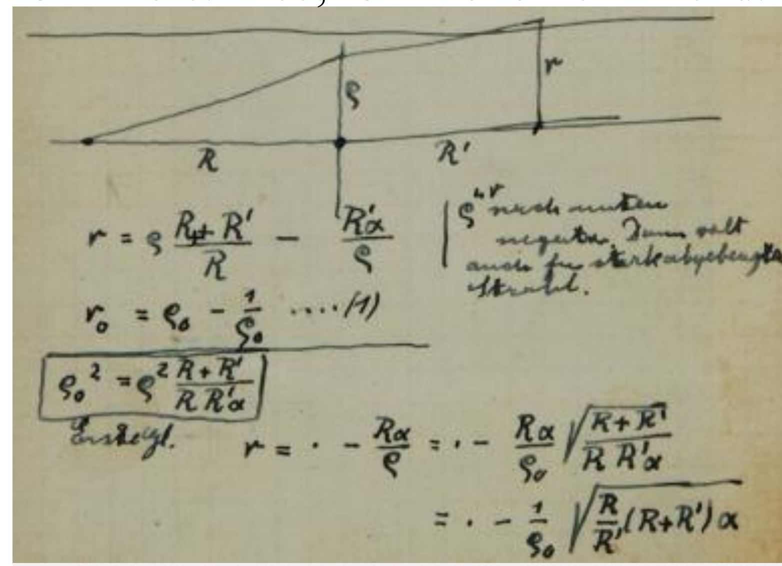

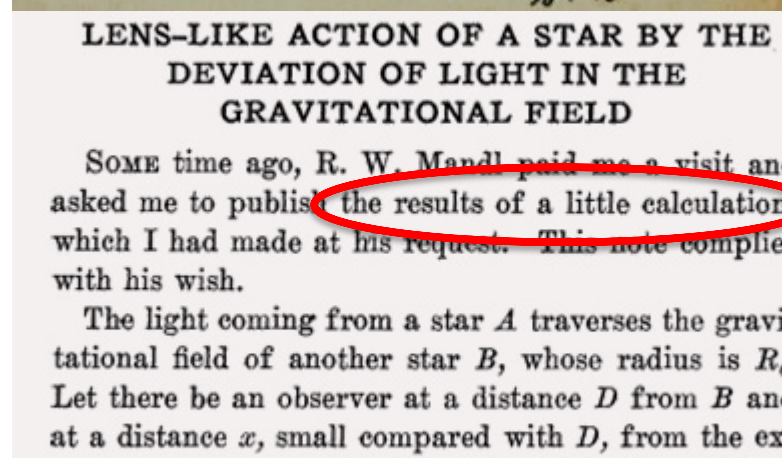

LENS-LIKE ACTION OF A STAR BY THE DEVIATION OF LIGHT IN THE GRAVITATIONAL FIELD

SOME time ago, R. W. Mandl paid me a visit and asked me to publish the results of a little calculation, which I had made at his request. This note complies with his wish.

The light coming from a star A traverses the gravitational field of another star B, whose radius is R_o. Let there be an observer at a distance D from B and at a distance x, small compared with D, from the ex-

1936, published paper on science.

- Pre-GR (e.g. 1912, Einstein's note)
- 1915, GR field equation
- 1919, Solar eclipse
  - **The magic number 2**

$$d\tau^2 = (1 + 2\Psi)dt^2 - (1 + 2\Phi)dX^2$$

Gravitational lensing

$$\boxed{\alpha = \frac{4GM}{c^2 b} = \frac{D_S}{D_{LS}}(\theta_I - \theta_S)}$$

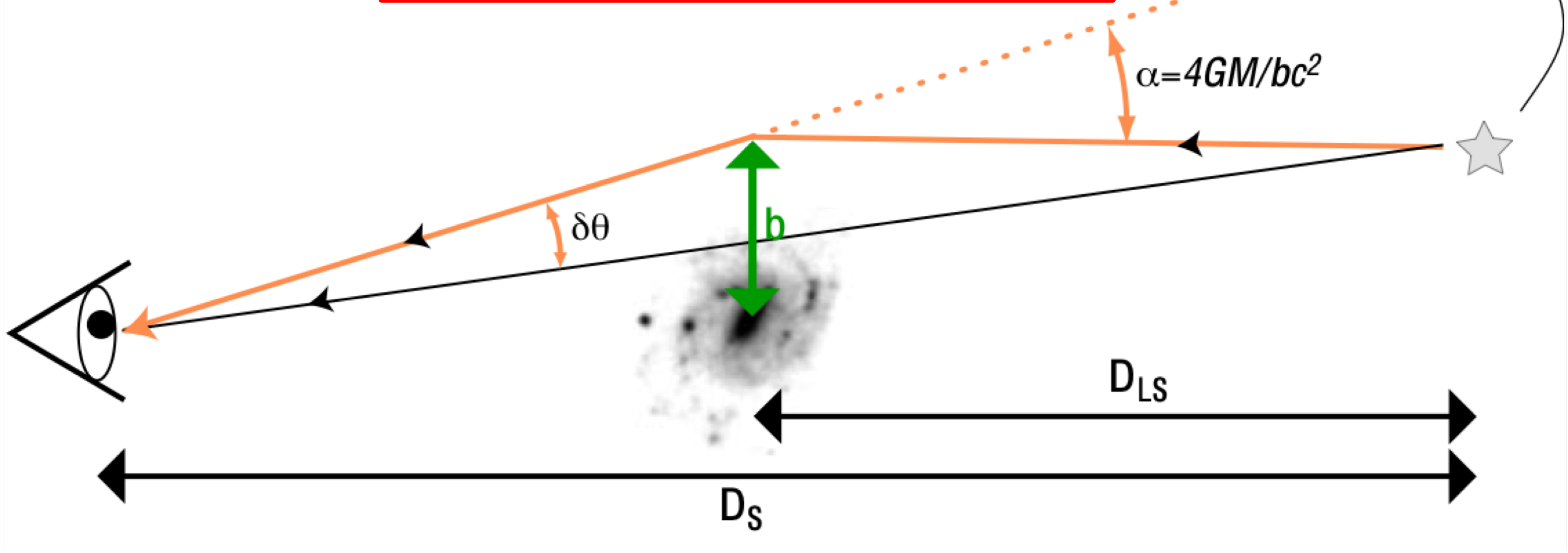

Gravitational lensing depends on the lens mass, distances to the lens/source and the lens-source distance

Strong lensing

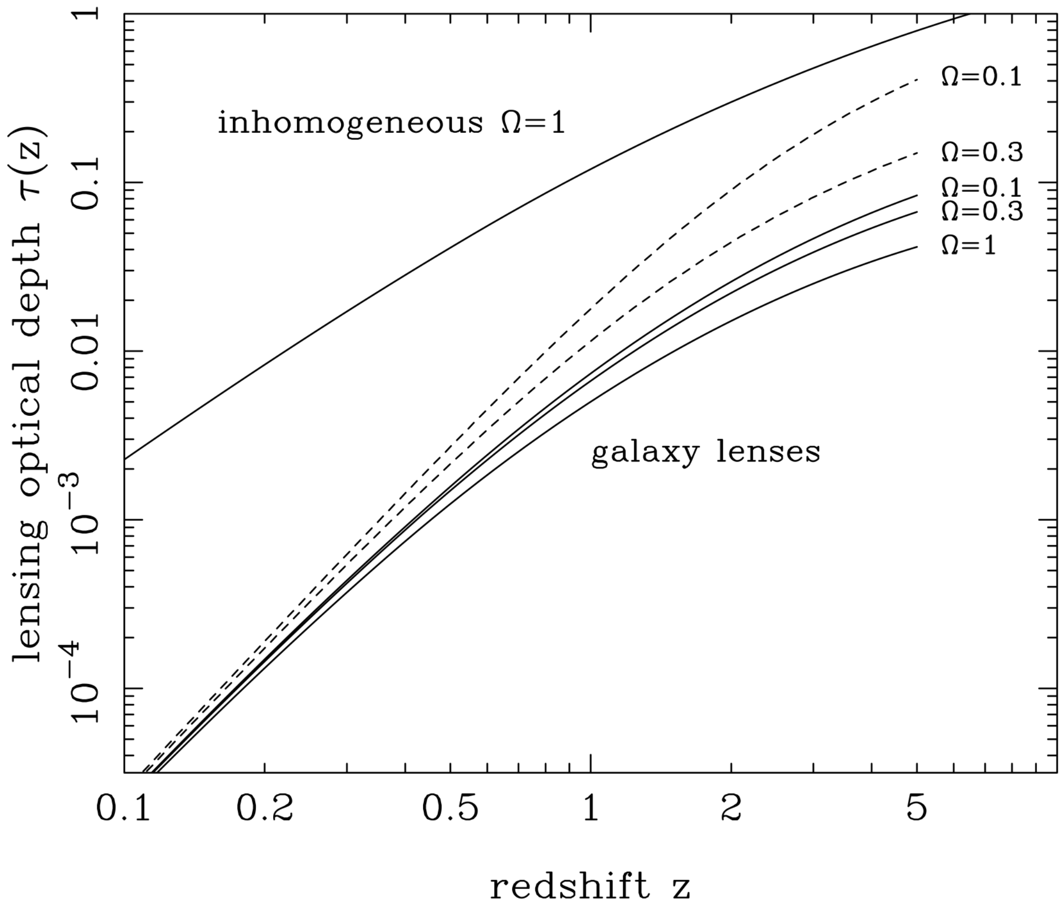

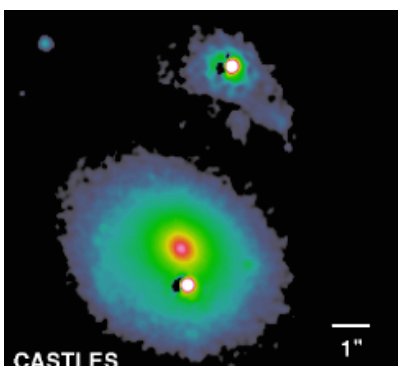

1979, the double quasar Q0957+561
Dennis Walsh, Robert F. Carswell and Ray J. Weymann

Weak lensing

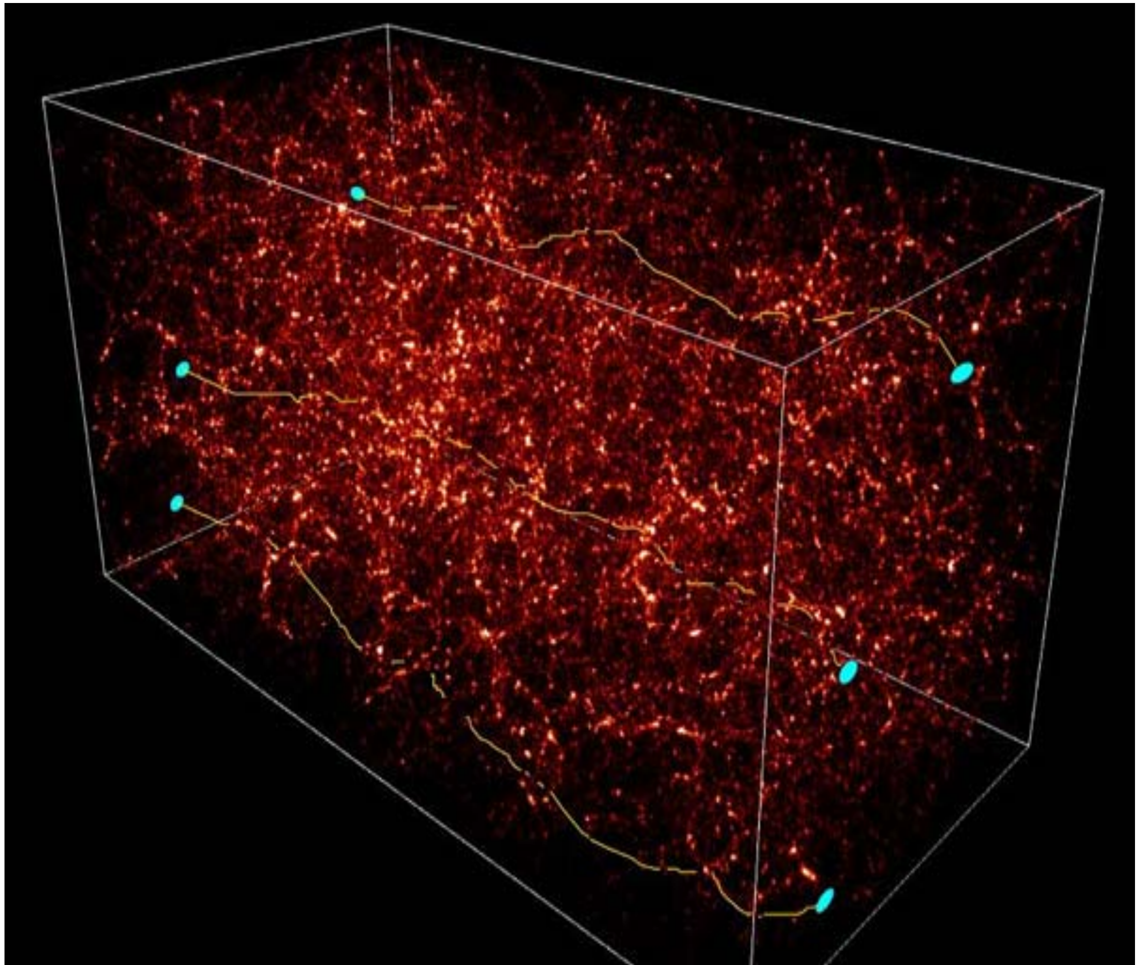

$$A_{ij} \equiv \frac{\partial \theta_S^i}{\partial \theta^j} \equiv \begin{pmatrix} 1-\kappa-\gamma_1 & -\gamma_2 \\ -\gamma_2 & 1-\kappa+\gamma_1 \end{pmatrix}$$

convergence shear

$$A_{ij} \equiv \frac{\partial \theta_S^i}{\partial \theta^j} \equiv \begin{pmatrix} 1-\kappa-\gamma_1 & -\gamma_2 \\ -\gamma_2 & 1-\kappa+\gamma_1 \end{pmatrix}$$

shear

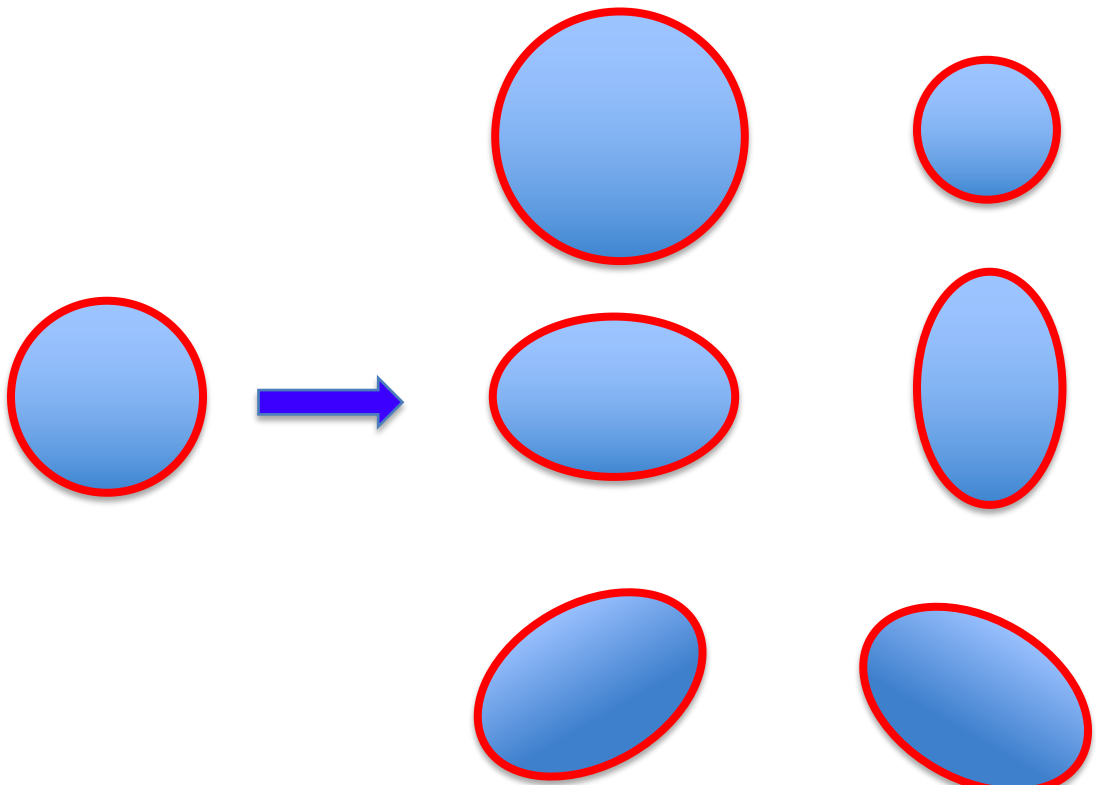

$\kappa \neq 0$

$\gamma_1 \neq 0$

$\gamma_2 \neq 0$

Weak lensing

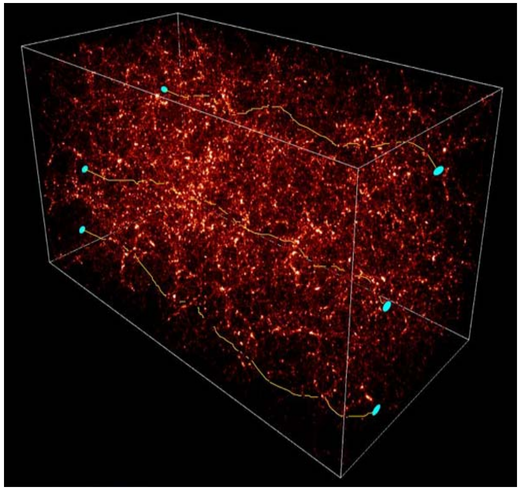

$$\frac{d^2x^\alpha}{d\lambda^2} + \Gamma^\alpha_{\mu\nu}\frac{dx^\mu}{d\lambda}\frac{dx^\nu}{d\lambda} = 0\ .$$

$$d\tau^2 = (1+2\Psi)dt^2 + a^2(1+2\Phi)dX^2$$

Position after lensing **real position on the sky** **Gravitational potential** **Geometry**

$$\theta^i_S = \theta^i_S + \int_0^{z_S} (\Psi - \Phi)_{,i} W(z_L, z_S) dz_L$$

$$= \theta^i_S + \int_0^{z_S} (2\Psi)_{,i} W(z_L, z_S) dz_L$$

e.g. *Modern cosmology* by Scott Dodelson

$$A_{ij} \equiv \frac{\partial \theta_S^i}{\partial \theta^j} \equiv \begin{pmatrix} 1-\kappa-\gamma_1 & -\gamma_2 \\ -\gamma_2 & 1-\kappa+\gamma_1 \end{pmatrix}$$

$$\kappa(\hat{n}) \propto \int \nabla^2 \Psi W(z_L, z_S) dz_L$$

$$\propto \int_0^{z_S} \delta_m(\hat{n}, z_L) W_L(z_L, z_S) dz_L$$

In the weak lensing regime, shear is fixed by convergence (leading order)

$$(\gamma_1, \gamma_2) \rightarrow (\gamma_E = \kappa, \gamma_B = 0)$$

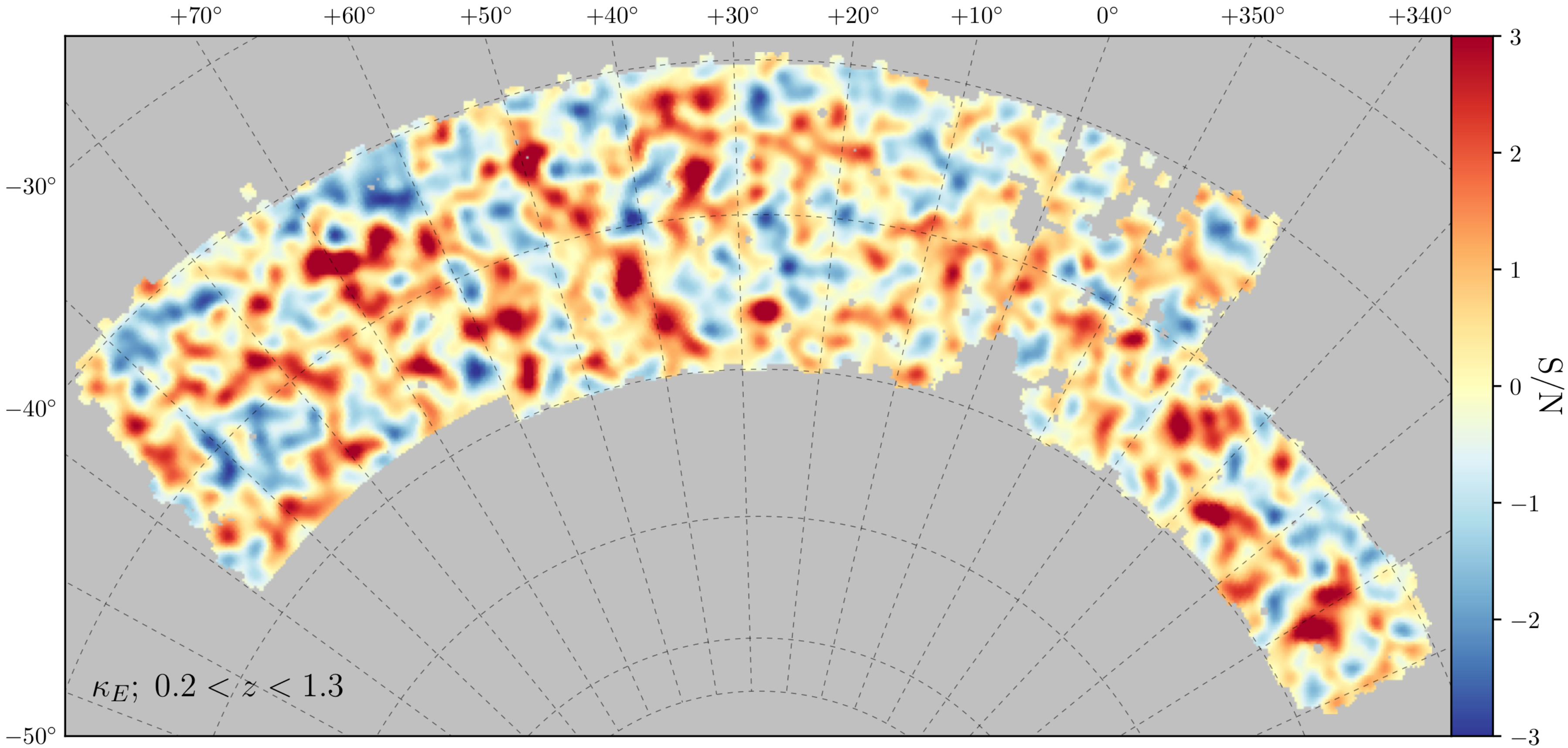

- DES Y1, 1708.01535

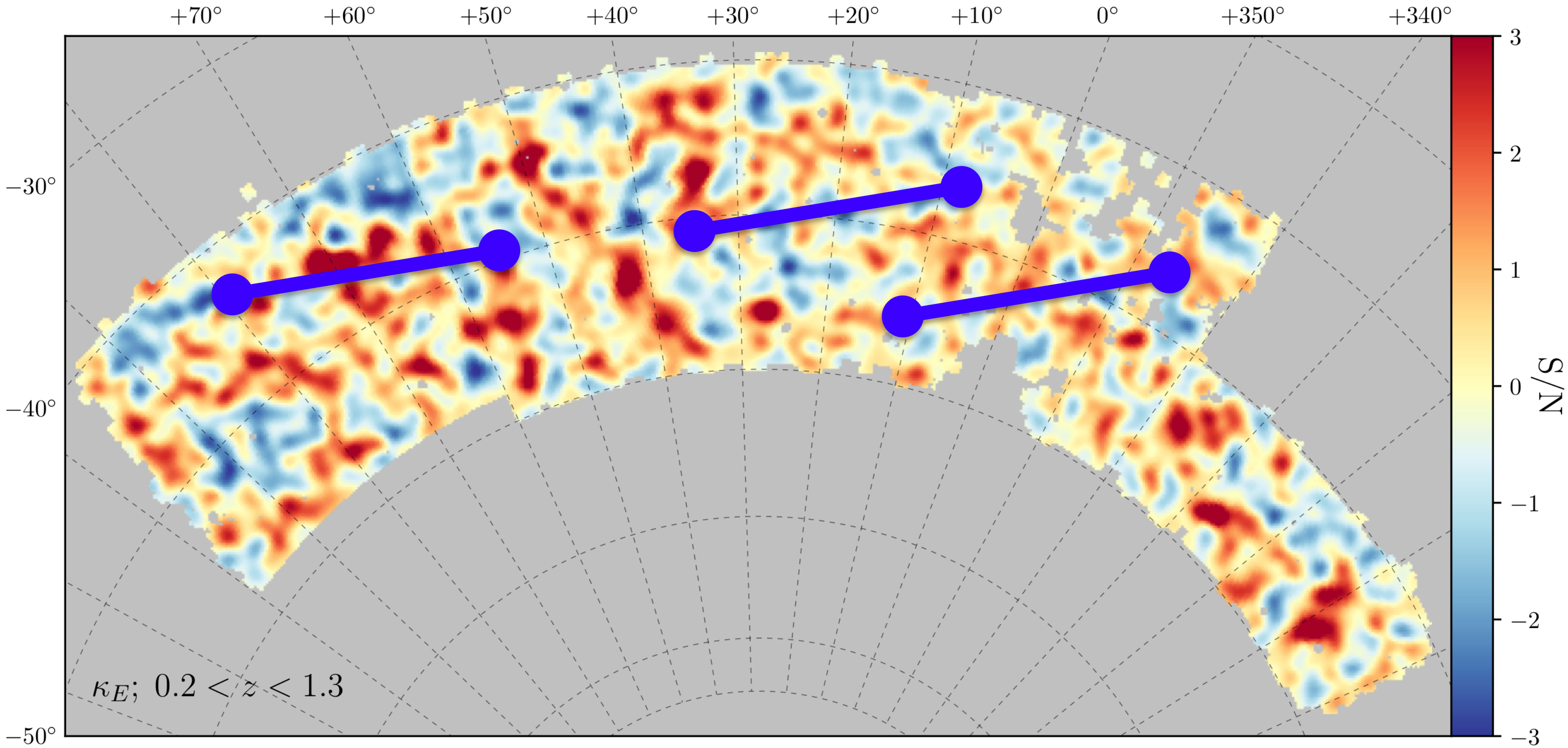

- DES Y1, 1708.01535

$$w(\theta) = \langle \kappa_1 \kappa_2 \rangle \quad C(\ell) = \langle |\kappa(\ell)|^2 \rangle$$

Weak lensing with tomography:

A major cosmological probe, with greatest potential!

$$\boxed{\frac{l^2 C_l}{2\pi}} = \frac{\pi}{l}\int_{observer}^{source} \boxed{\Delta^2\left(k=\frac{l}{x_L}, z_i\right)} \boxed{D^2\left(k=\frac{l}{x_L}, z\right)} \boxed{W^2(x_L, x_S)} dz_L$$

Angular power spectrum+higher order

Measurable

Initial fluctuations (cosmic origin)

(Nonlinear) growth factor -> neutrino, DM, DE, gravity

Lensing geometry-> expansion rate->DM, DE, gravity

Weak lensing tomography

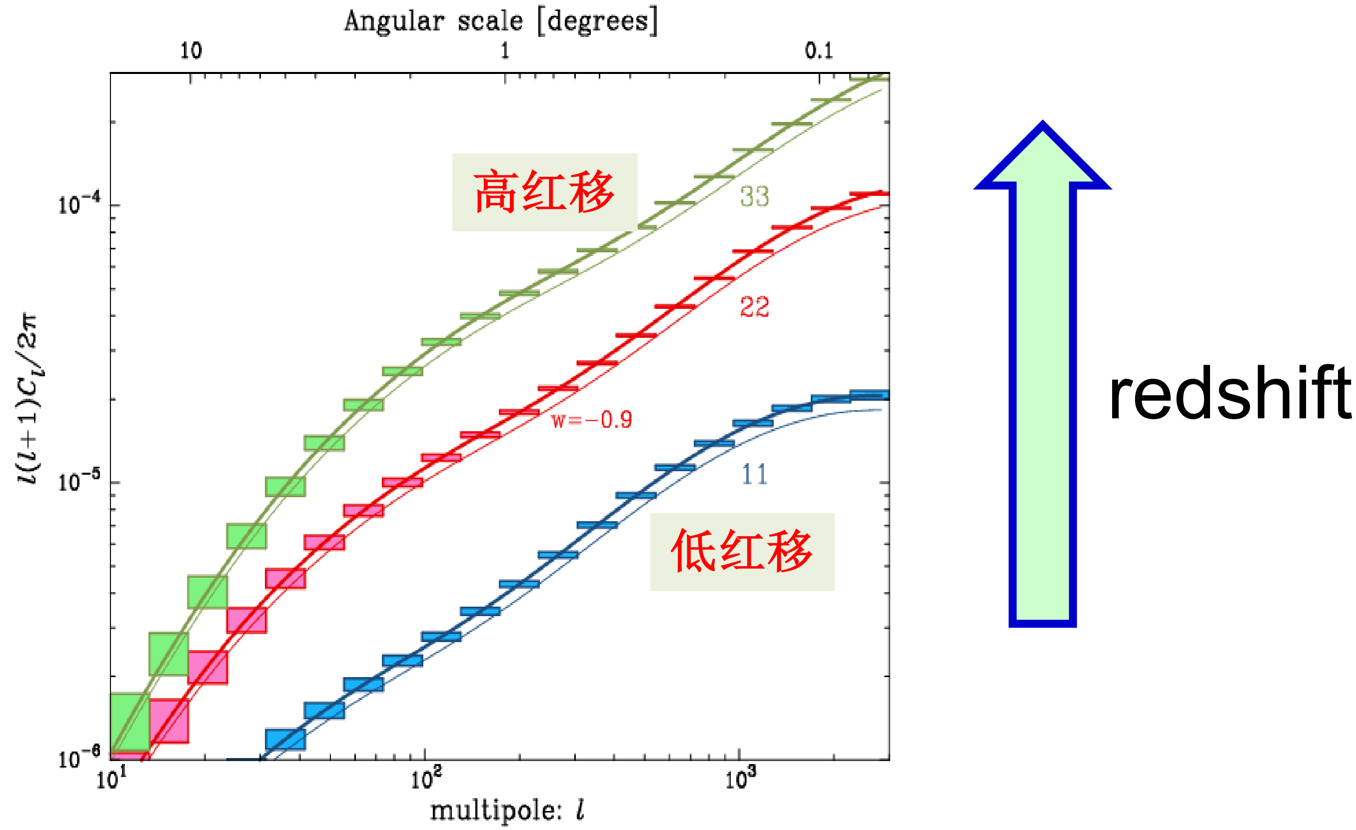

Figure 14.3: The lensing power spectra constructed from galaxies split into three broad redshift bins: $z < 0.7, 0.7 < z < 1.2$, and $1.2 < z < 3$. The solid curves are predictions for the fiducial ΛCDM model and include nonlinear evolution. The boxes show the expected measurement error due to the sample variance and intrinsic ellipticity errors (see text for details). The thin curves are the predictions for a dark energy model with $w = -0.9$. Clearly such a model can be distinguished at very high significance using information from all bins in ℓ and z. Note that many more redshift bins are expected from LSST than shown here, leading to over a hundred measured auto- and cross-power spectra.

Great potentials

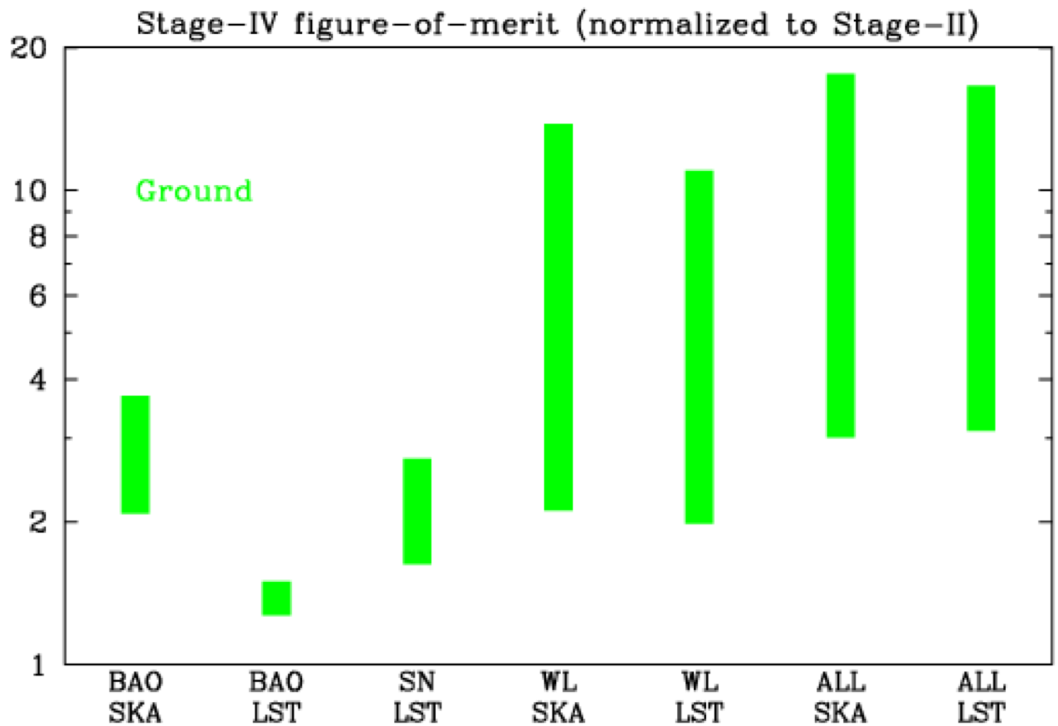

- Dark Energy Task force
- FoM: joint constraint on dark energy EoS

$$w(a) = w_0 + w_a(1 - a)$$

Approaches of
weak lensing measurement

- **Cosmic shear** $\leftarrow \gamma$
- **Cosmic magnification** $\leftarrow \kappa$
- **Lensing of cosmic backgrounds** $\leftarrow \kappa\ ,\ \gamma$

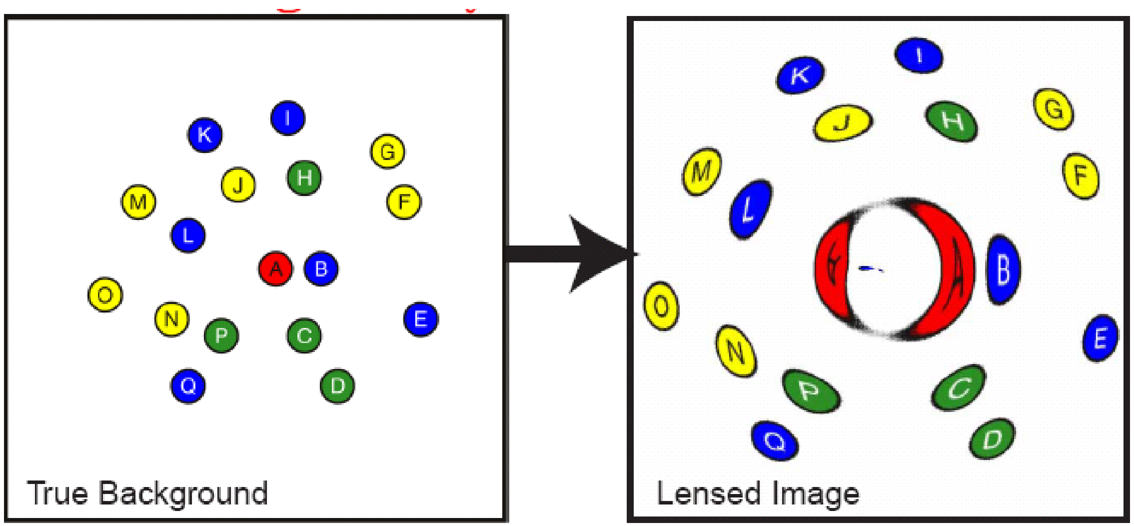

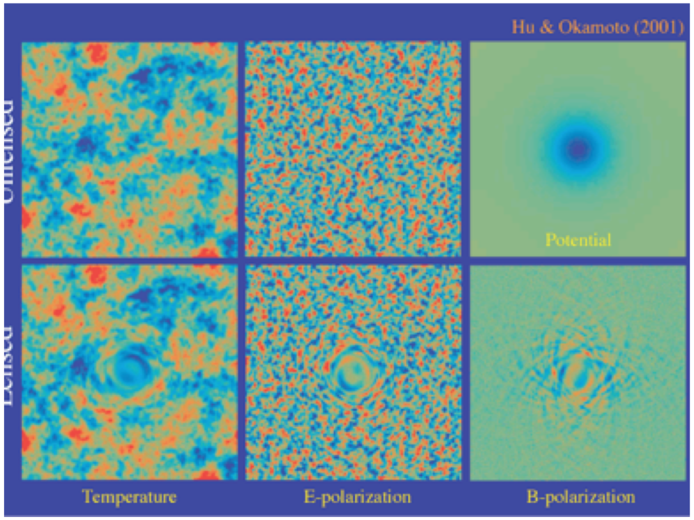

Weak lensing measurements: cosmic shear

$$\epsilon_1 \equiv \frac{q_{xx} - q_{yy}}{q_{xx} + q_{yy}}$$

$$\epsilon_i \rightarrow \epsilon_i + 2\gamma_i$$

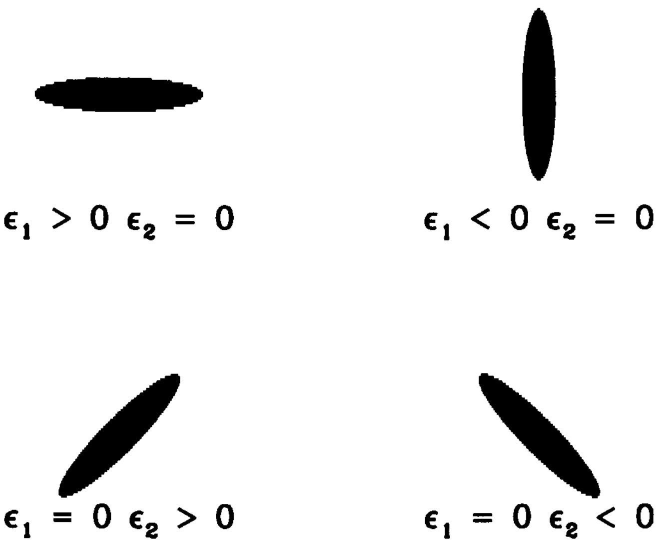

$$\epsilon_2 \equiv \frac{2q_{xy}}{q_{xx} + q_{yy}}.$$

Larger, deeper, wider

- **-2000: N_g=O(10^5)**
- **2000s: N_g=O(10^7): CFHTLenS, SDSS, COSMOS, RCSLenS, etc.**
- **2010s: N_g=O(10^8): KiDS, DES, HSC,**
- **2020s: N_g=O(10^9): CSST, Euclid, LSST, WFIRST, +**

Wittman+, 2000

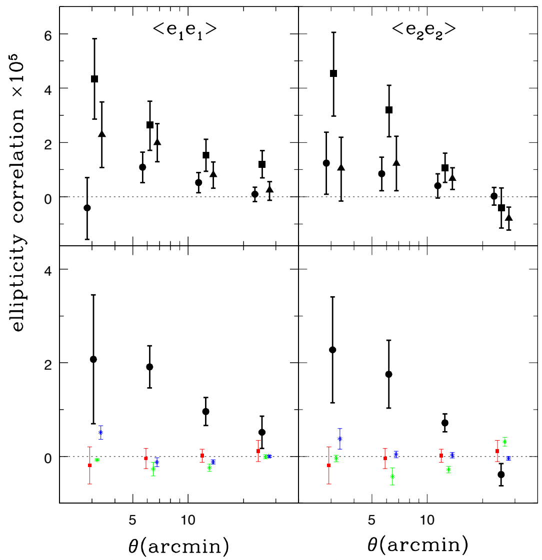

HSC: Hikage+, 2018

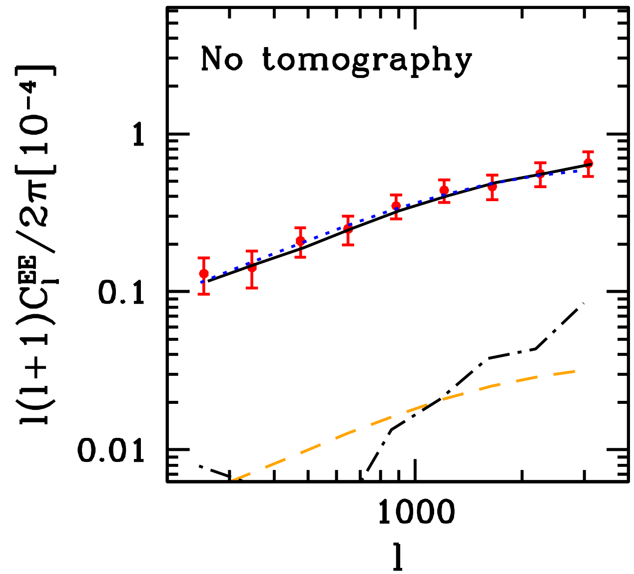

CFHTLenS, Fu+ 2014

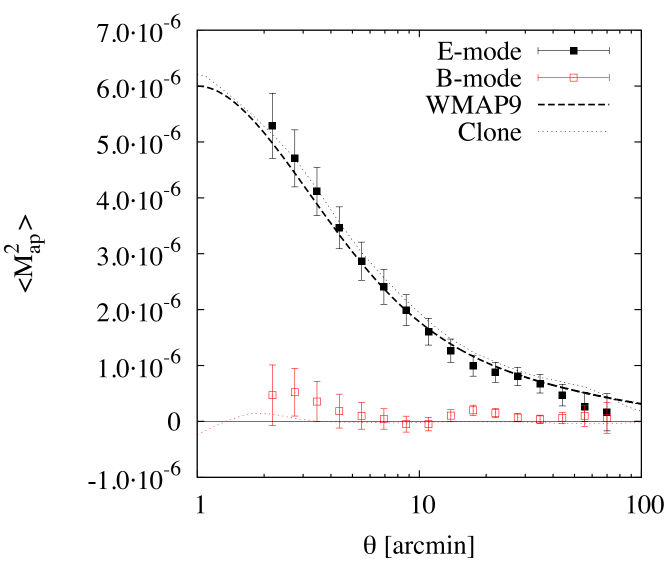

DES: Troxel+, 2017

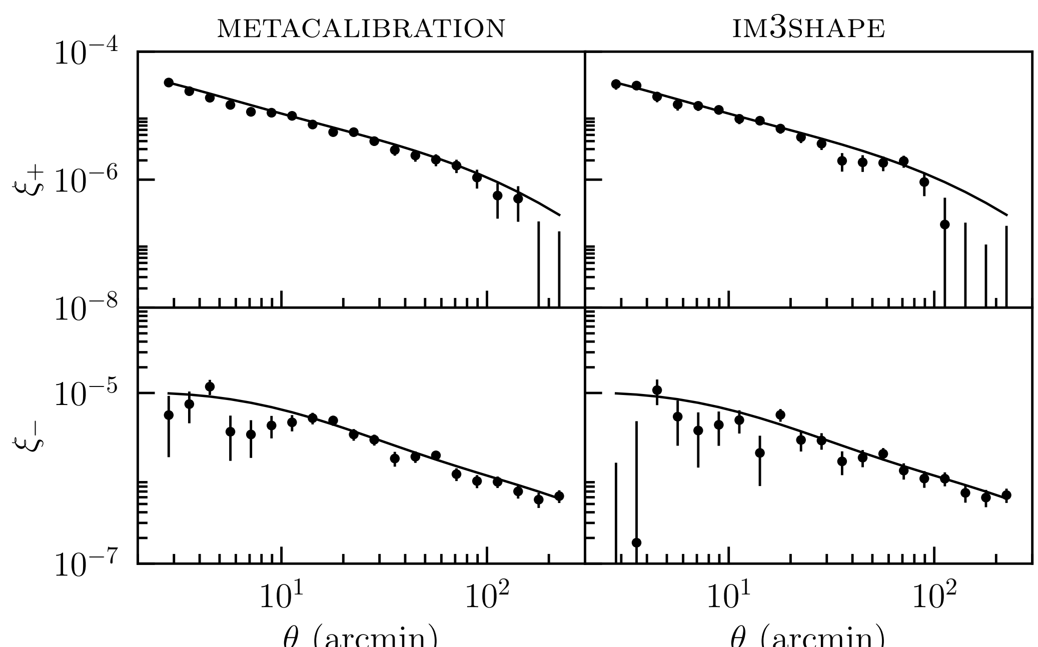

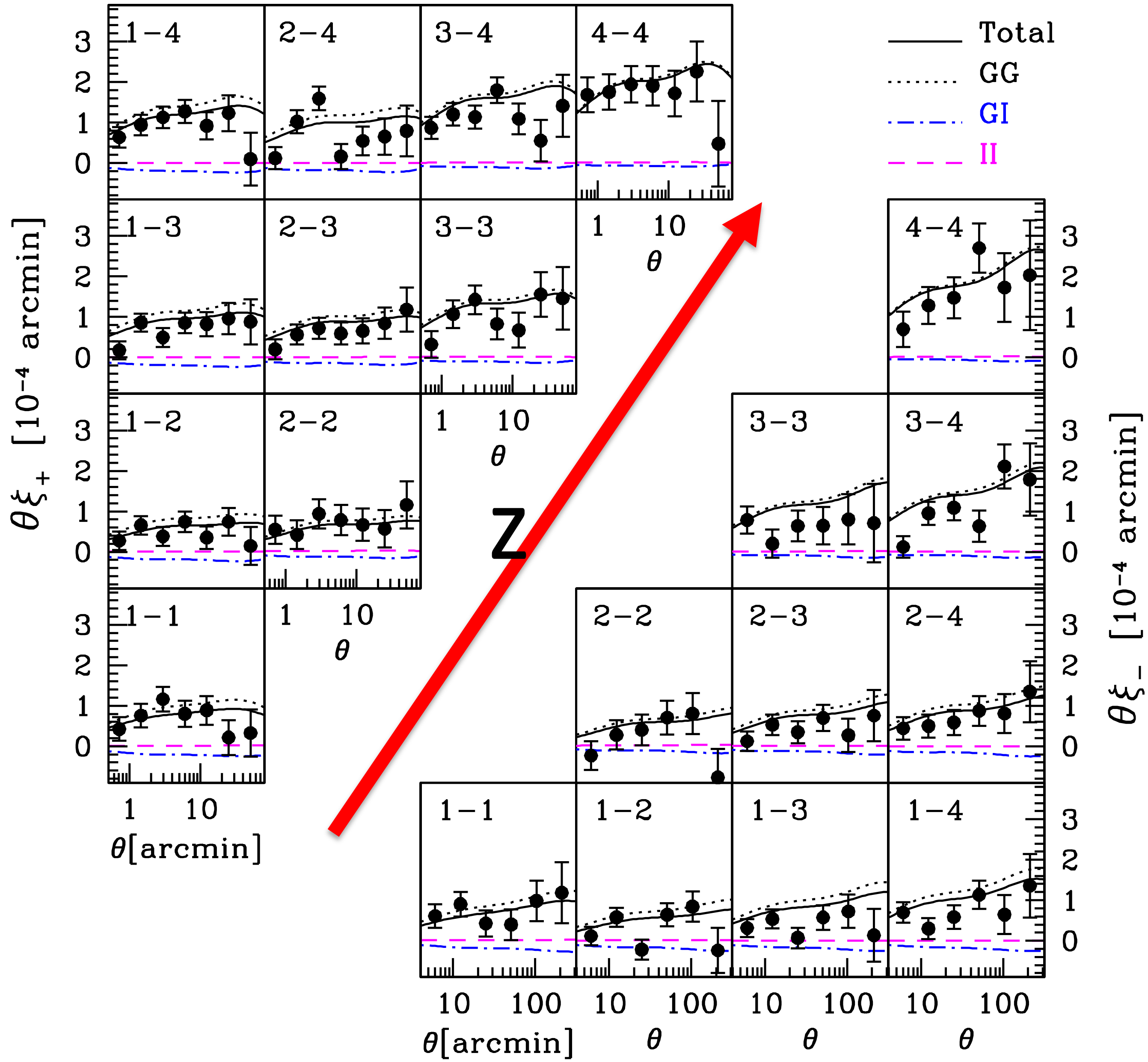

KiDS-450. Hildebrandt +, 2016

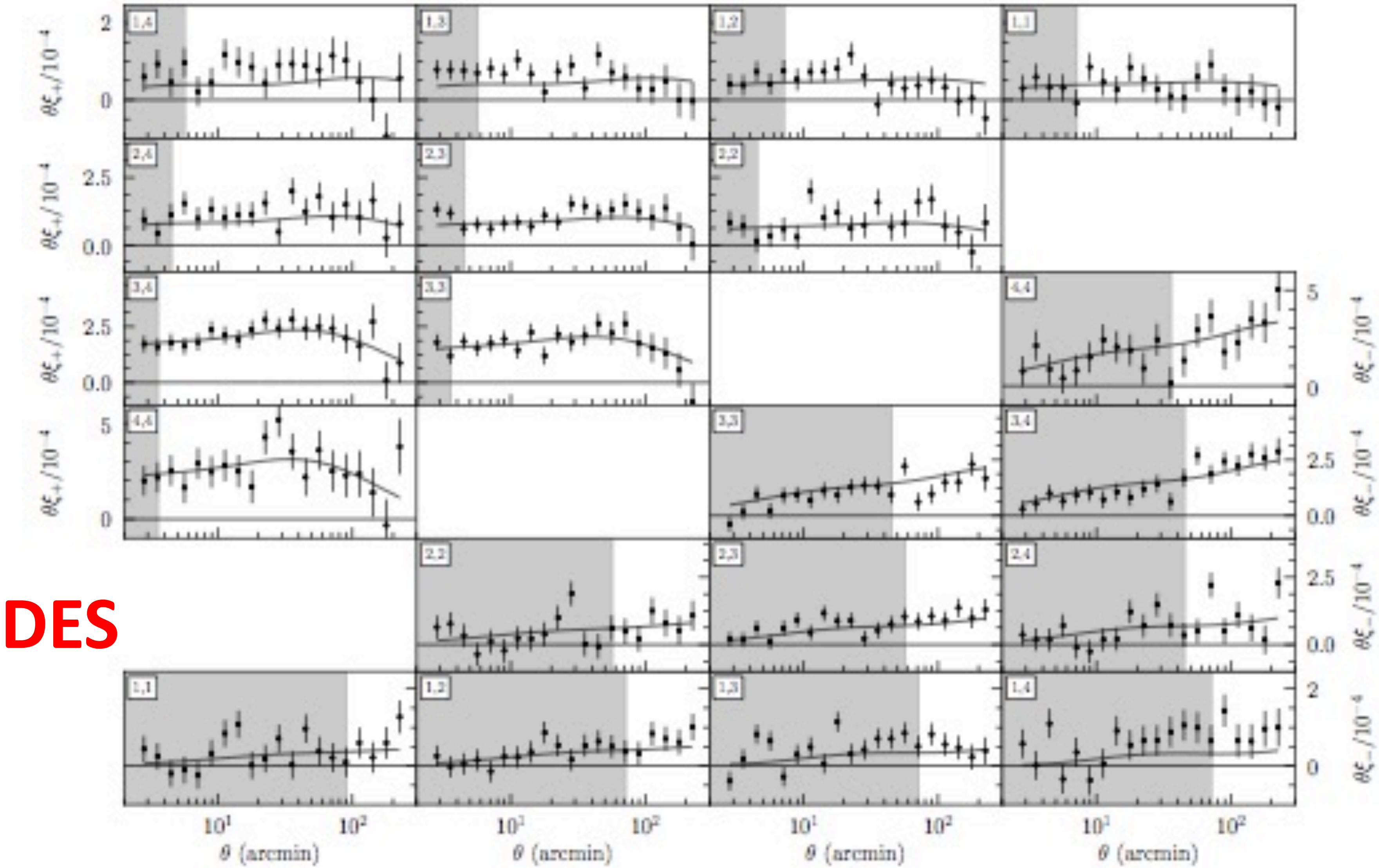

FIG. 4. The measured shear correlation function ξ_+ (top triangle) and ξ_- (bottom triangle) for the DES Y1 METACALIBRATION catalog. Results are scaled by the angular separation (θ) to emphasize features and differences relative to the best-fit model. The correlation functions are measured in four tomographic bins spanning the redshift ranges listed in Table I, with labels for each bin combination in the upper left corner of each panel. The assignment of galaxies to tomographic bins is discussed in Sec. II B. Scales which are not used in the fiducial analysis are shaded (see Sec. VII A). The best-fit ΛCDM theory line from the full tomographic analysis is shown as the solid line. We find a χ^2 of 227 for 211 degrees of freedom in the non-shaded regions.

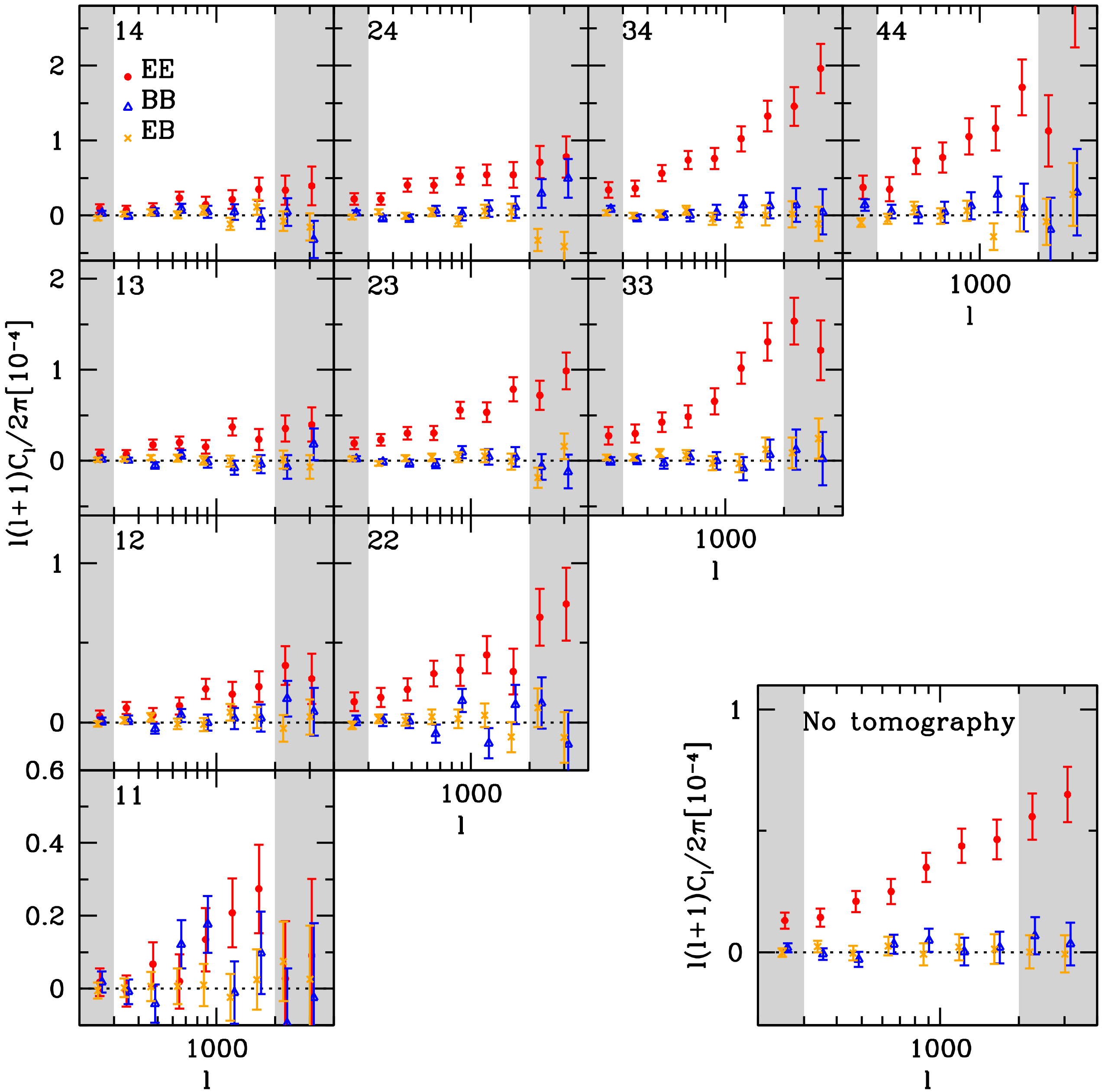
14
24
34
44
13
23
33
12
22
11
EE
BB
EB
No tomography
l(l+1)C_l/2π[10^-4]
l
1000

HSC

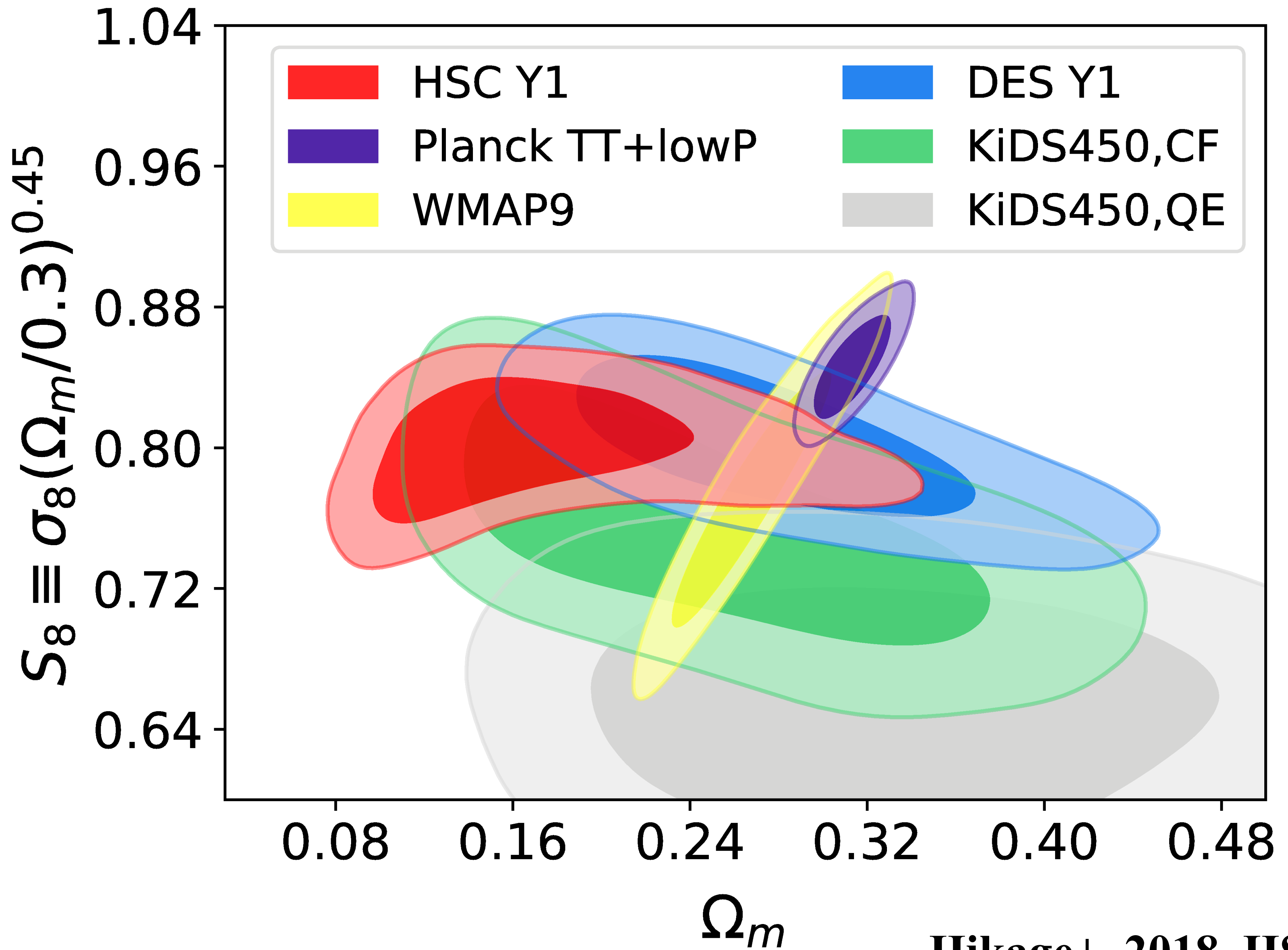

Hikage+, 2018. HSC

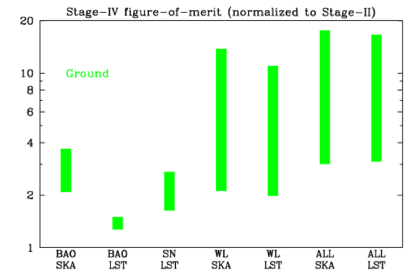

- **But 20 years after the first detections, cosmic shear surveys still can not detect dark energy independently**

- **In contrast, BAO (2005-) already confirmed the existence of dark energy independent of any other methods.**

Precise ≠ accurate!

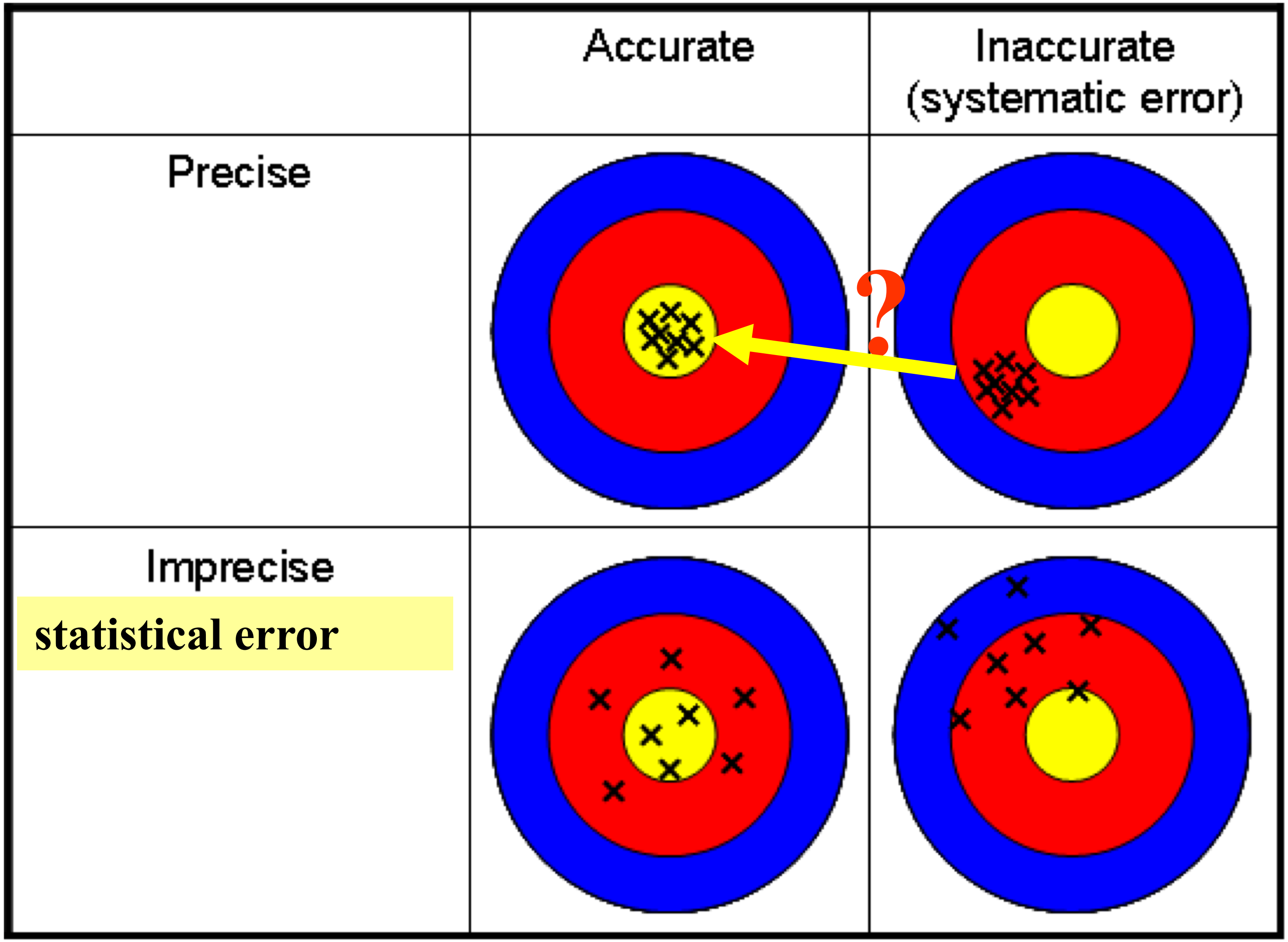

Challenges to cosmic shear cosmology

- **Systematic errors in observational measurement**
  - **Galaxy shape measurement (e.g. GREAT3 test)**
  - **Galaxy intrinsic alignment (e.g. Troxel et al. 2015 review)**
  - **Photo-z error (in particular outliers)**
  - **Other knowns and unknowns (e.g. LSST science book)**

- **Systematic errors in theoretical modeling**
  - **Baryon effects (non-gravitational processes such as gas cooling, SN and AGN feedback, etc.)**
  - **Nonlinear and non-Gaussian evolution**
  - **Second order corrections: source-lens clustering, Born deviation, lens-lens coupling, reduced shear, etc.**

One example: baryonic effect

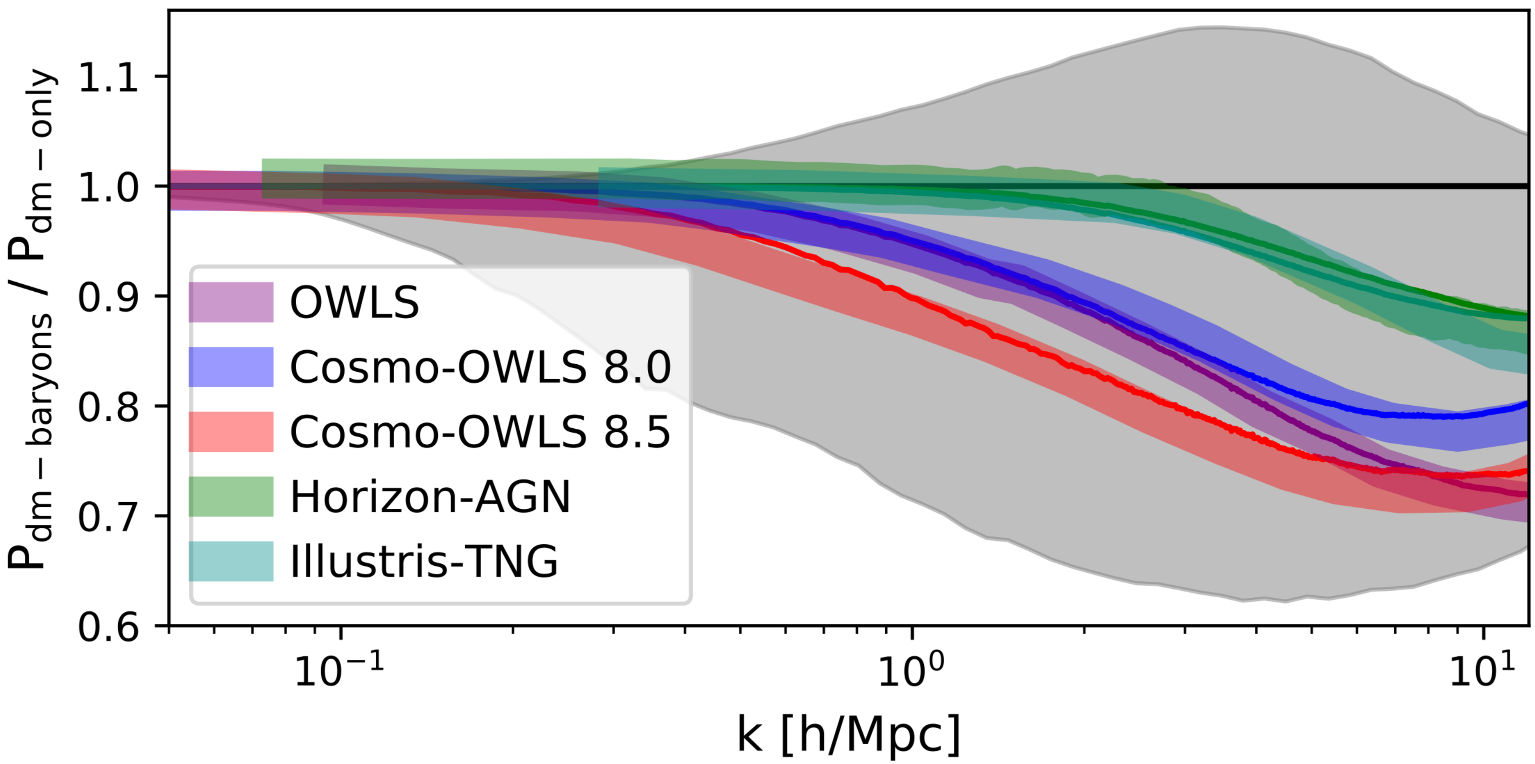

Schneider+ 1910.11357

Challenges to cosmic shear cosmology

- **Systematic errors in observational measurement**
  - **Galaxy shape measurement (e.g. GREAT3 test)**
  - **Galaxy intrinsic alignment (e.g. Troxel et al. 2015 review)**
    - **ZPJ 2010a; 2010b; Meng+ 2018; Yao+ 2019,2020**
  - **Photo-z error (in particular outliers)**
    - **ZPJ+ 2010; Le Zhang+ 2016**
  - **Other knowns and unknowns (e.g. LSST science book)**
- **Magnification:** **ZPJ & Pen 2005, 2006; Yang & ZPJ 2011; Yang+ 2015; 2017; ZPJ+2018; ZPJ+ 2019**
- **Systematic errors in theoretical modeling**
  - **Baryon effects (non-gravitational processes such as gas cooling, SN and AGN feedback, etc.).** **Jing, ZPJ+ 2006**
  - **Nonlinear and non-Gaussian evolution**
    - **Yu+ 2011, 2012, 2016; Liu+ 2020; Chen+ 2020; Qin+ 2020**
  - **Second order corrections: source-lens clustering, Born deviation, lens-lens coupling, reduced shear, etc.** **Yu+ 2015**

Galaxy intrinsic alignment

- Galaxy intrinsic alignment could mean
  - Galaxy number distribution aligned with something
  - **Galaxy shape aligned with something. Spatially correlated**

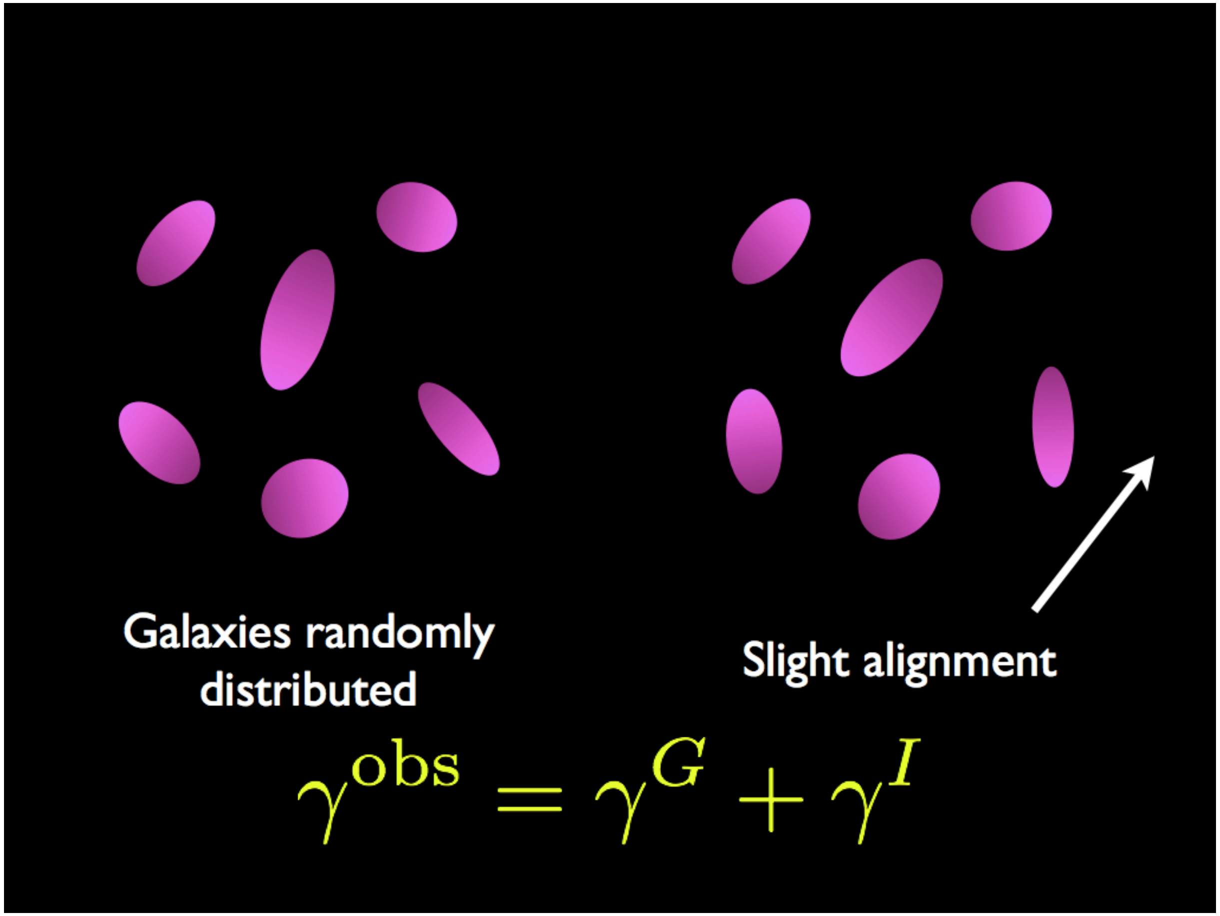

Impact on weak lensing statistics

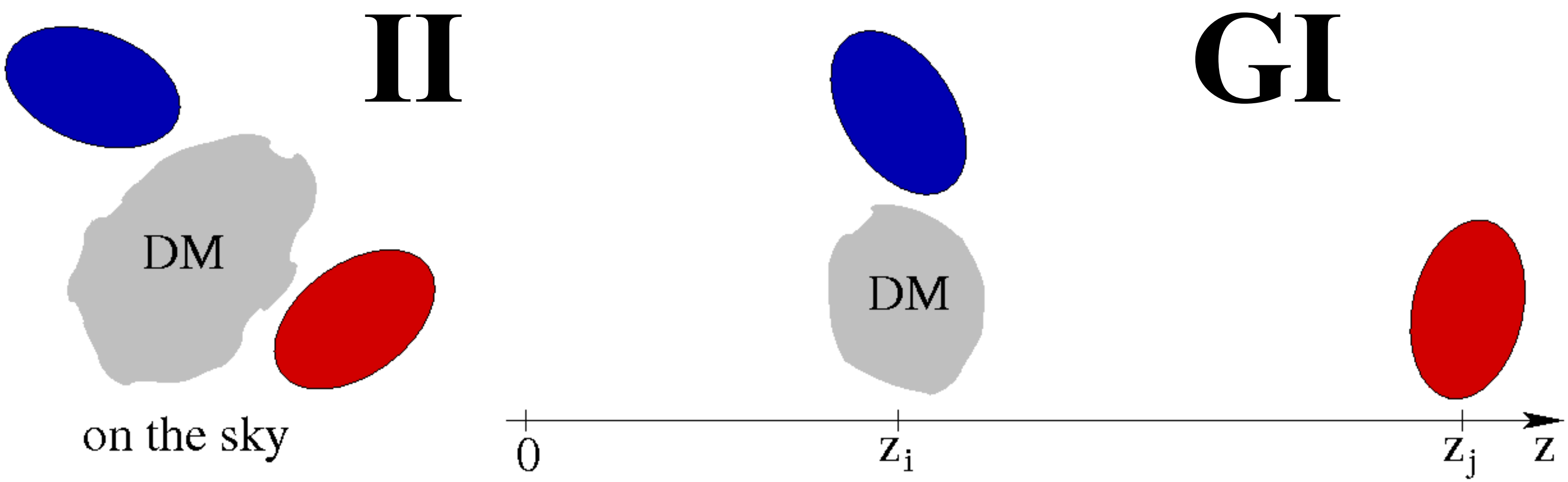

$$w^{\mathrm{obs}} = \langle (\gamma^G(a) + \gamma^I(a))(\gamma^G(b) + \gamma^I(b)) \rangle$$
$$= GG + II + GI$$

II/GI in simulations and theoretical models

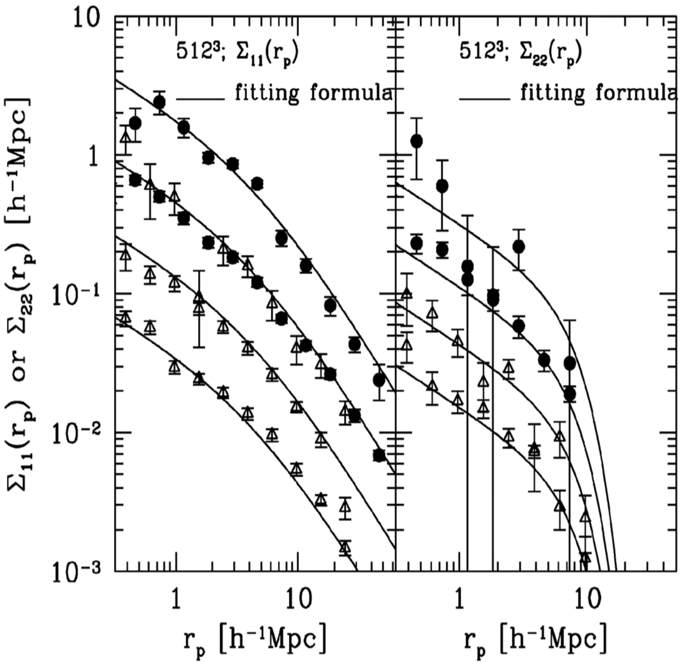

Jing 2002

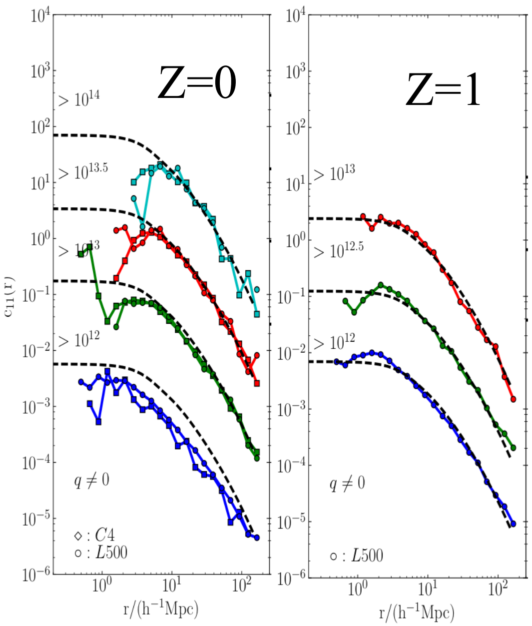

Xia+ 2017

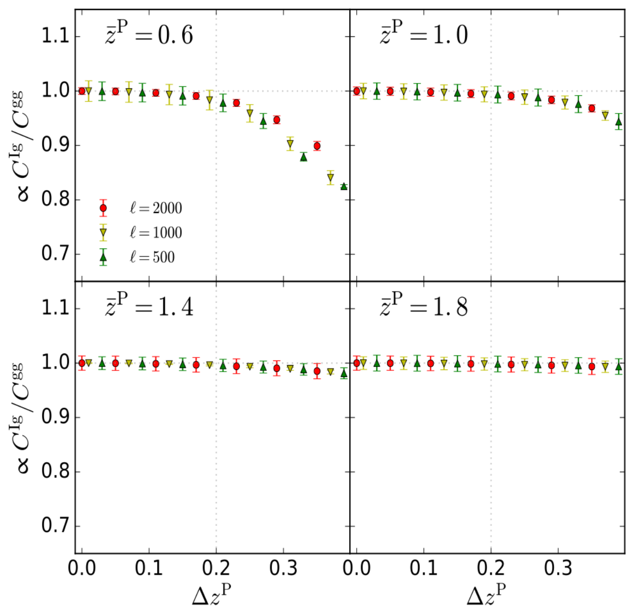

Meng+ 2018

Linear alignment model

- **Hirata & Seljak, 2004**

With bias correction

- **Xia+ 2017**

$$\boxed{\gamma^I_{(t,\times)} = -\frac{C_1}{4\pi G}(\nabla_x^2 - \nabla_y^2, 2\nabla_x\nabla_y)S[\Psi_P]}$$

II and GI in observations

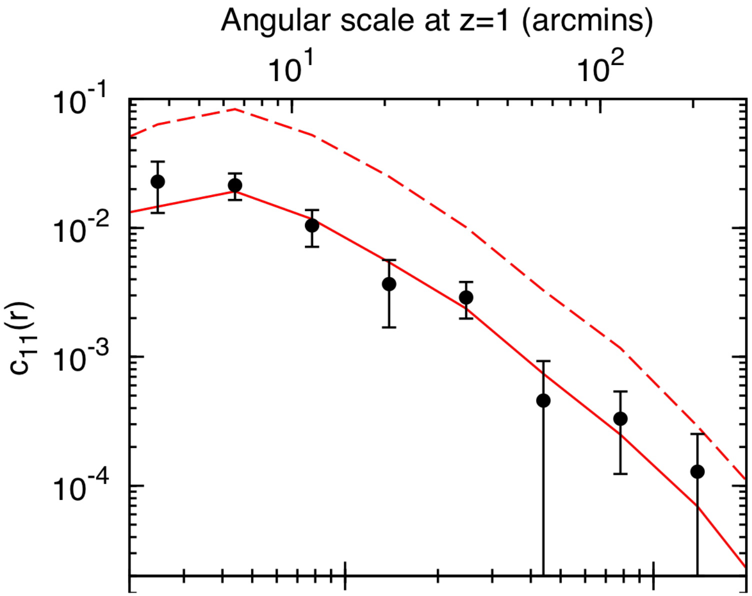

Okumura+ 2009

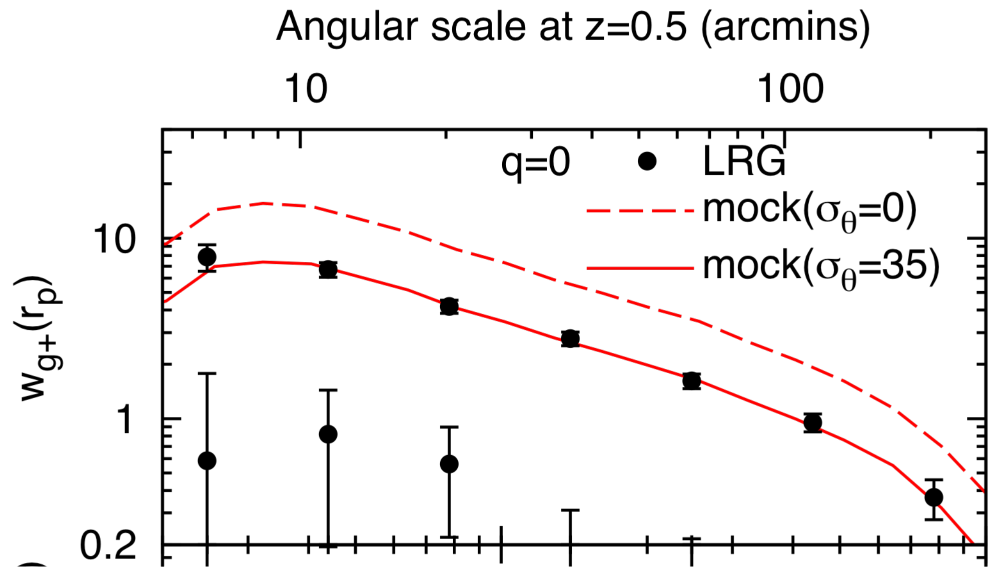

Okumura & Jing 2009

Halo 1 **Halo 2**

$$f(\theta;\sigma_\theta)d\theta = \frac{1}{\sqrt{2\pi}\sigma_\theta}\exp\left[-\frac{1}{2}\left(\frac{\theta}{\sigma_\theta}\right)^2\right]d\theta,$$

$$\sigma_\theta = 35.4^{+4.0}_{-3.3}\ \mathrm{deg}$$

Intrinsic alignment

- Depend on galaxy properties (types, color, luminosity, etc) and redshift
- May have different origins (early/late)
- Many models （each with multiple nuisance parameters)
- Significant bias in cosmological constraints

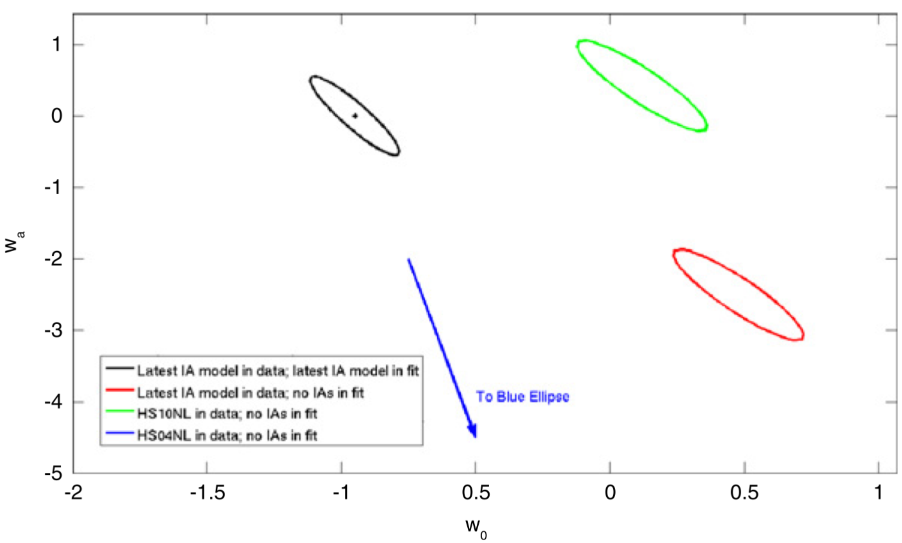

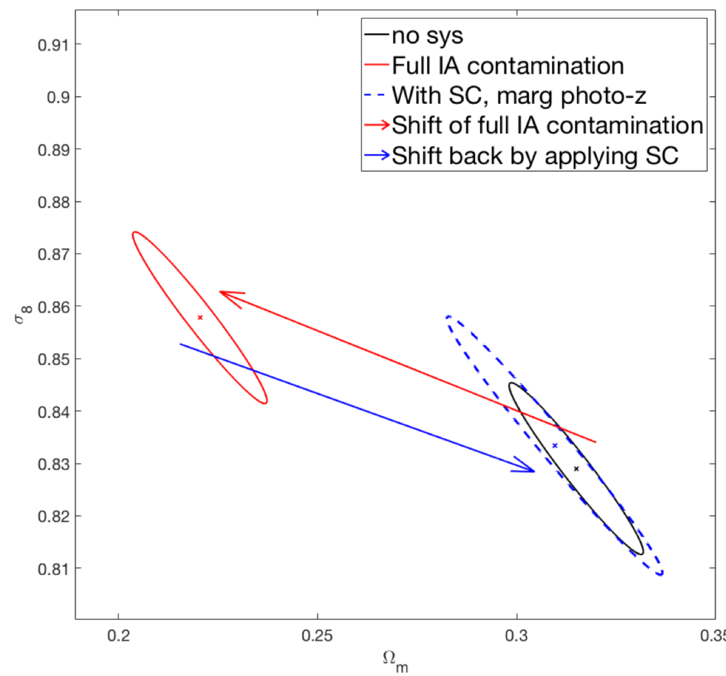

Kirk+ 2012

Yao+ 2017

Mitigating Intrinsic alignment in cosmic shear surveys

- Template fitting (adopted in most data analysis)
  - with model dependence
- Nulling in redshift space (Joachimi & Schneider 2008, 2009)
  - but loss of information
- Self-calibrations to separate G and I model indepdently
  - ZPJ 2010a, Yao+ 2019, Yao+2020; ZPJ 2010b, Meng+ 2018
  - Flip over galaxy pair, compare density-shape correlation, separate G/I

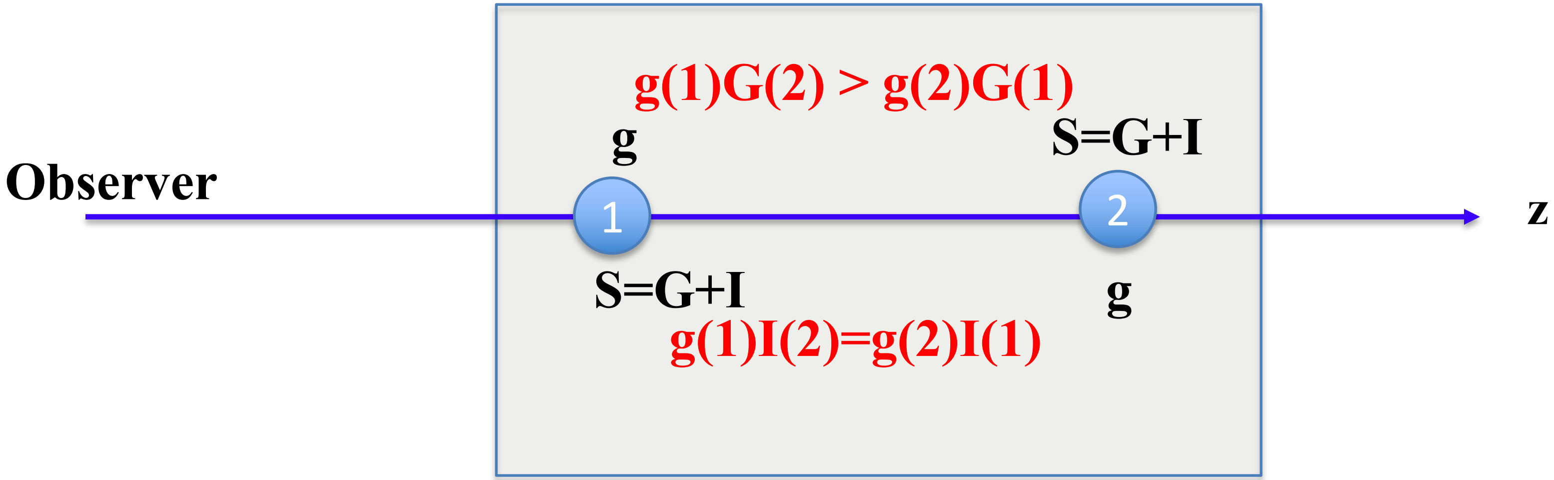

Same photo-z bin

First application: KiDS450/KV450
Yao Ji(姚骥)+ 2019
15M, 450 deg^2, 0.1<z<0.9

G+I

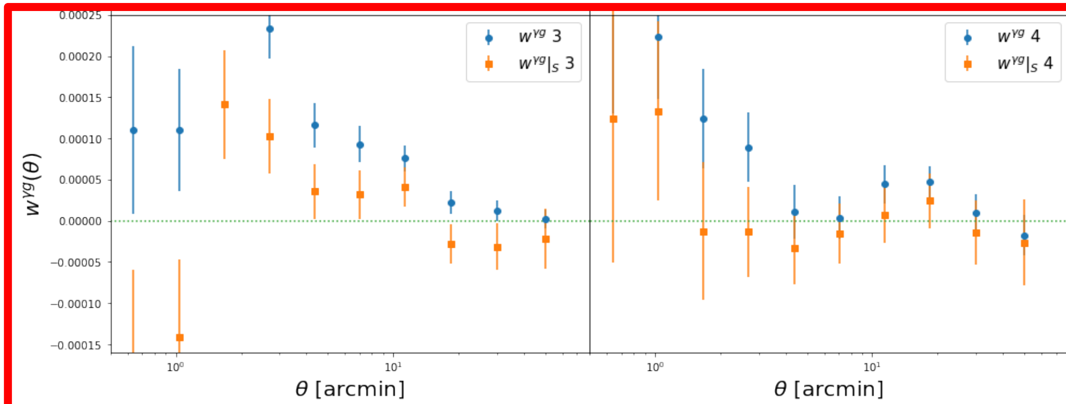

$4 - 9\sigma$

G

I

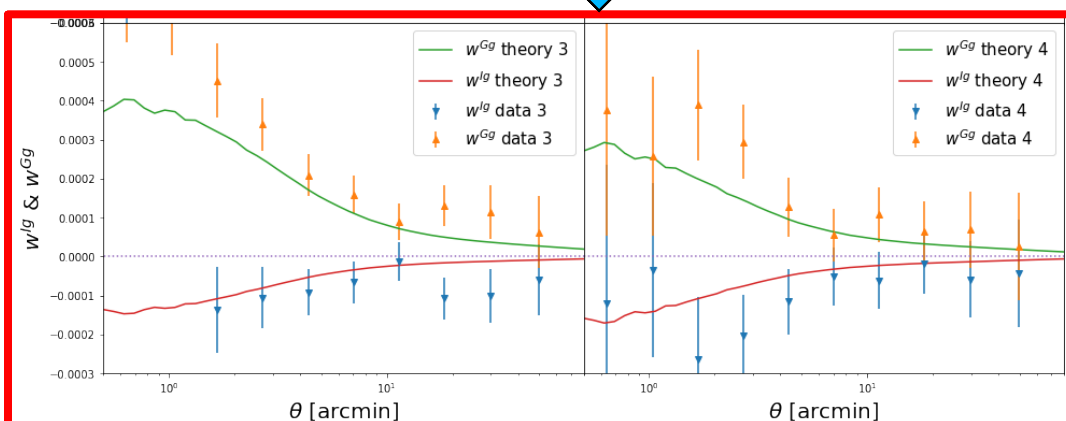

Application to DECaLS DR3
23M, 4200 deg^2 (g,r,z), $0.1<z^P<0.9$

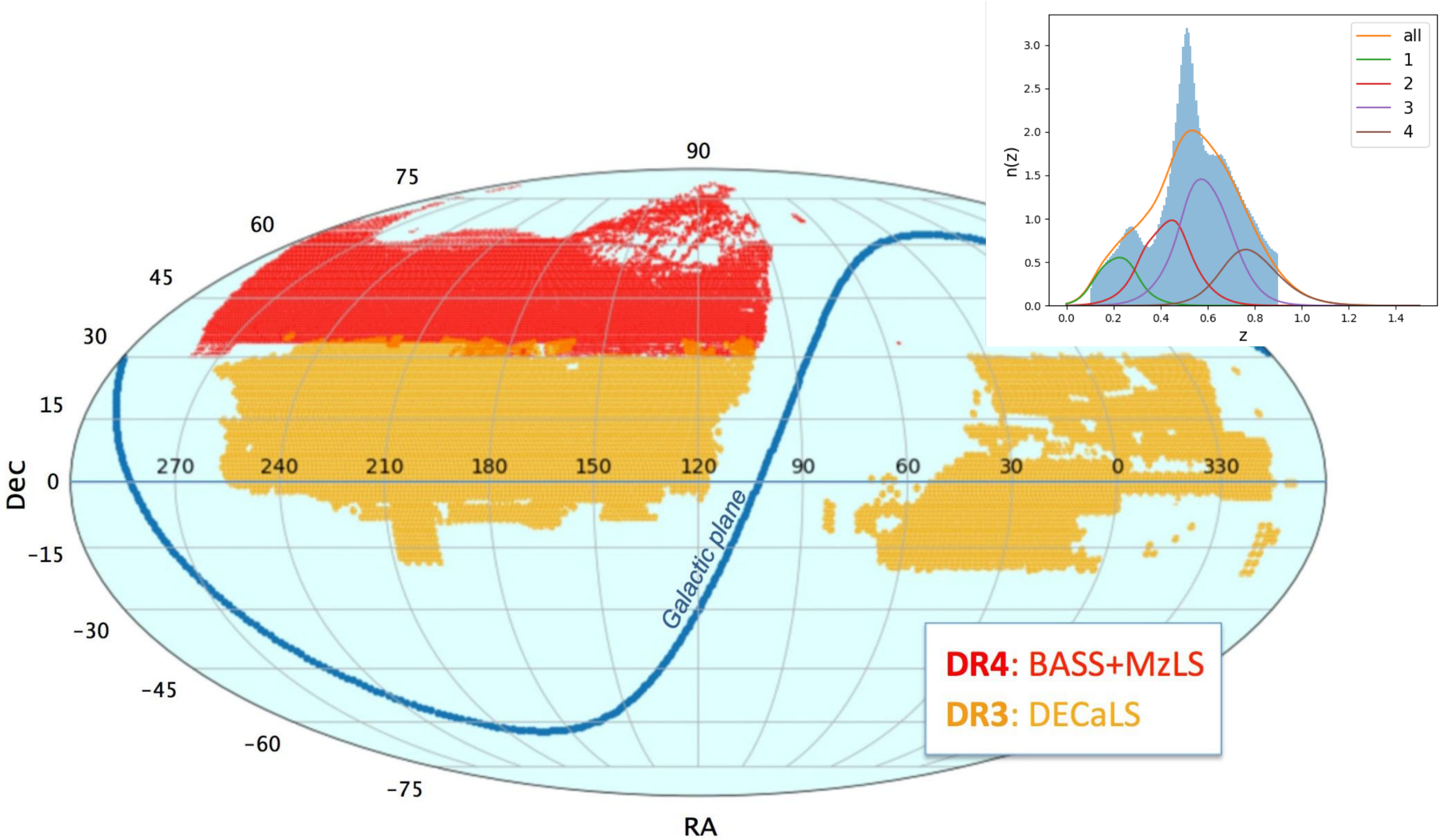

Application to DECaLS

$$(3.7\sigma,\ 20\sigma,\ 15\sigma,\ 5.9\sigma)$$

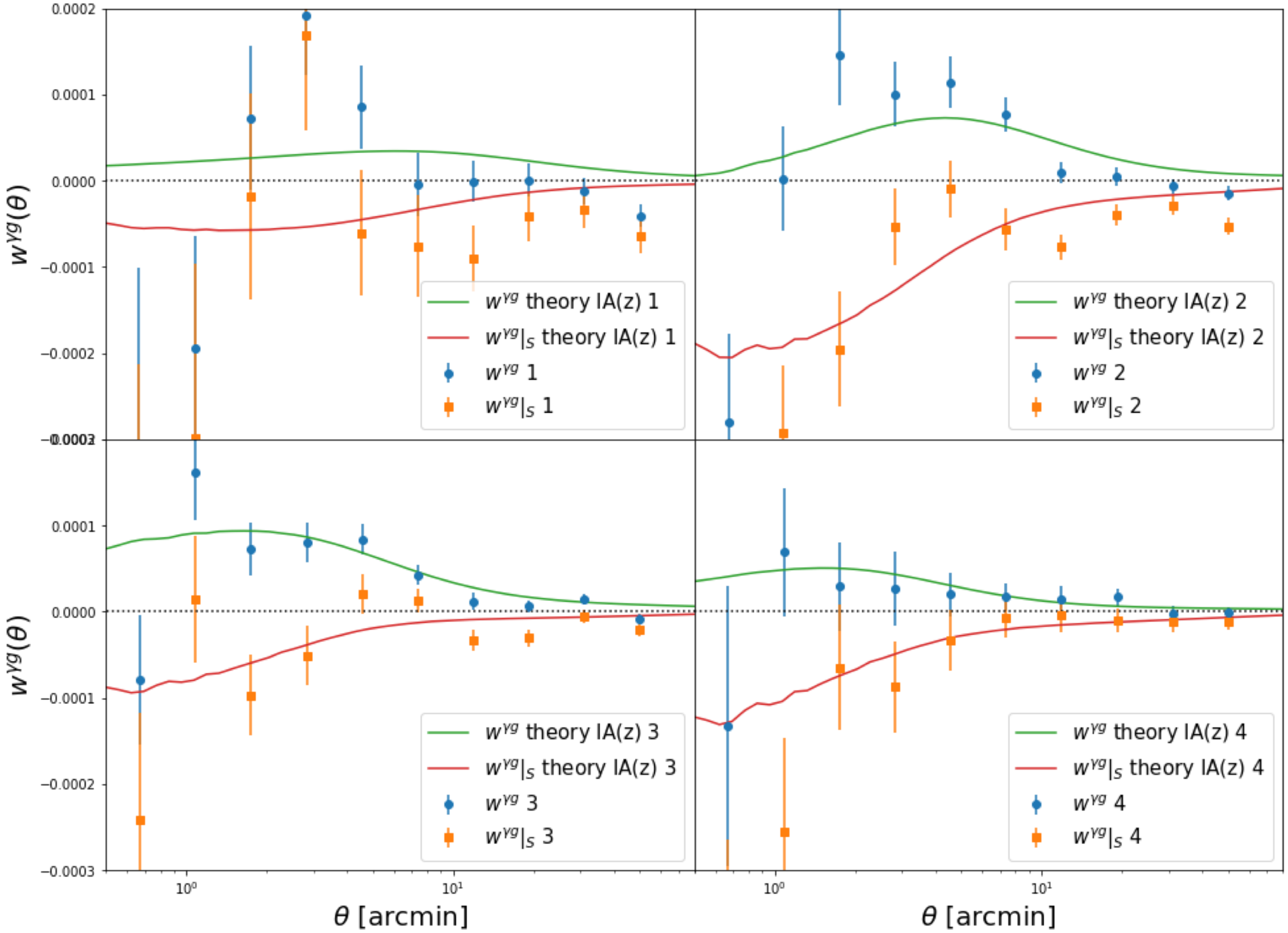

Application to DECaLS

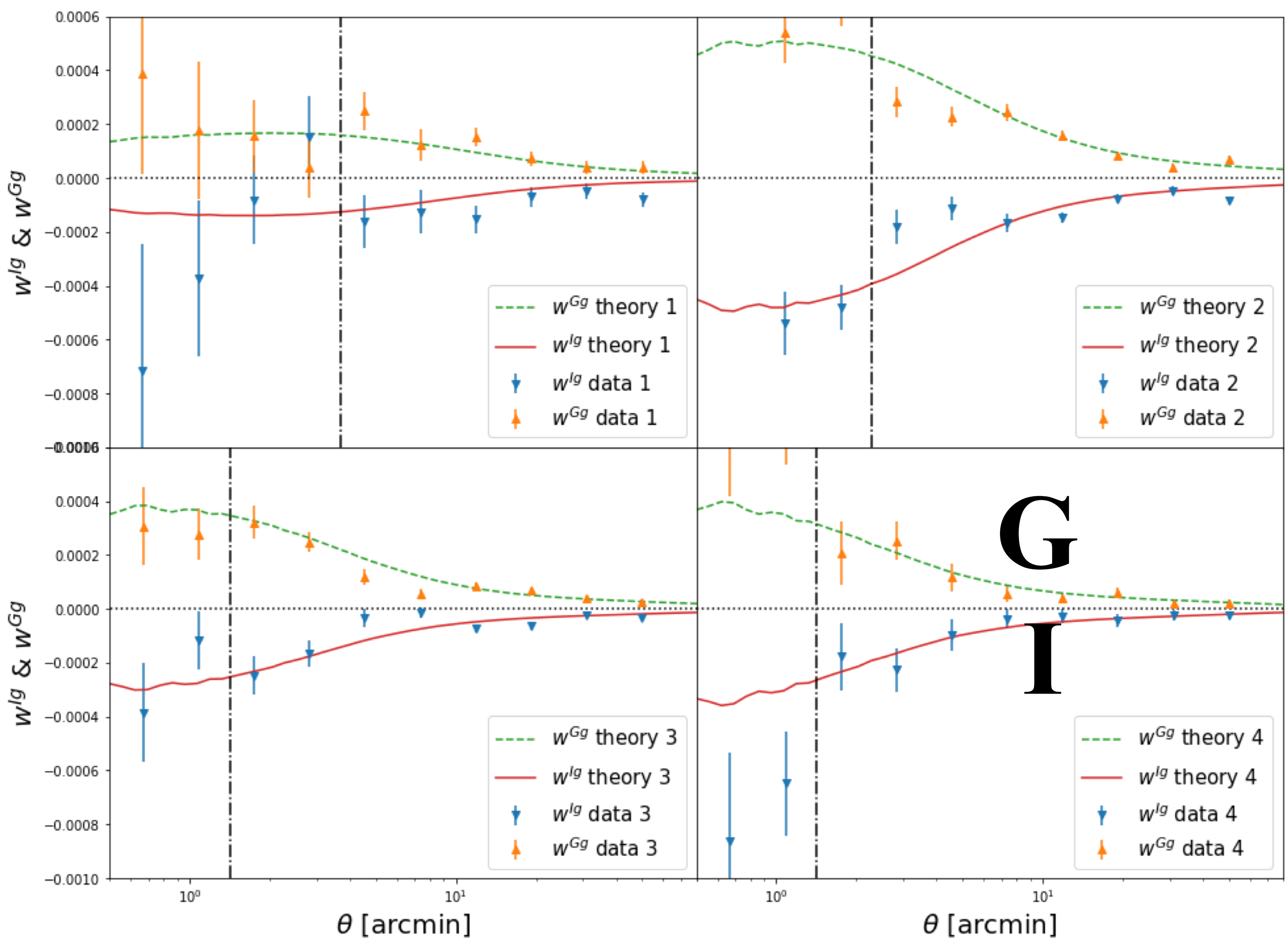

Application to DECaLS: red galaxies

$$S/N=6.6,\ 22,\ 12,\ 9.2$$

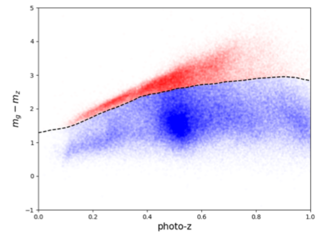

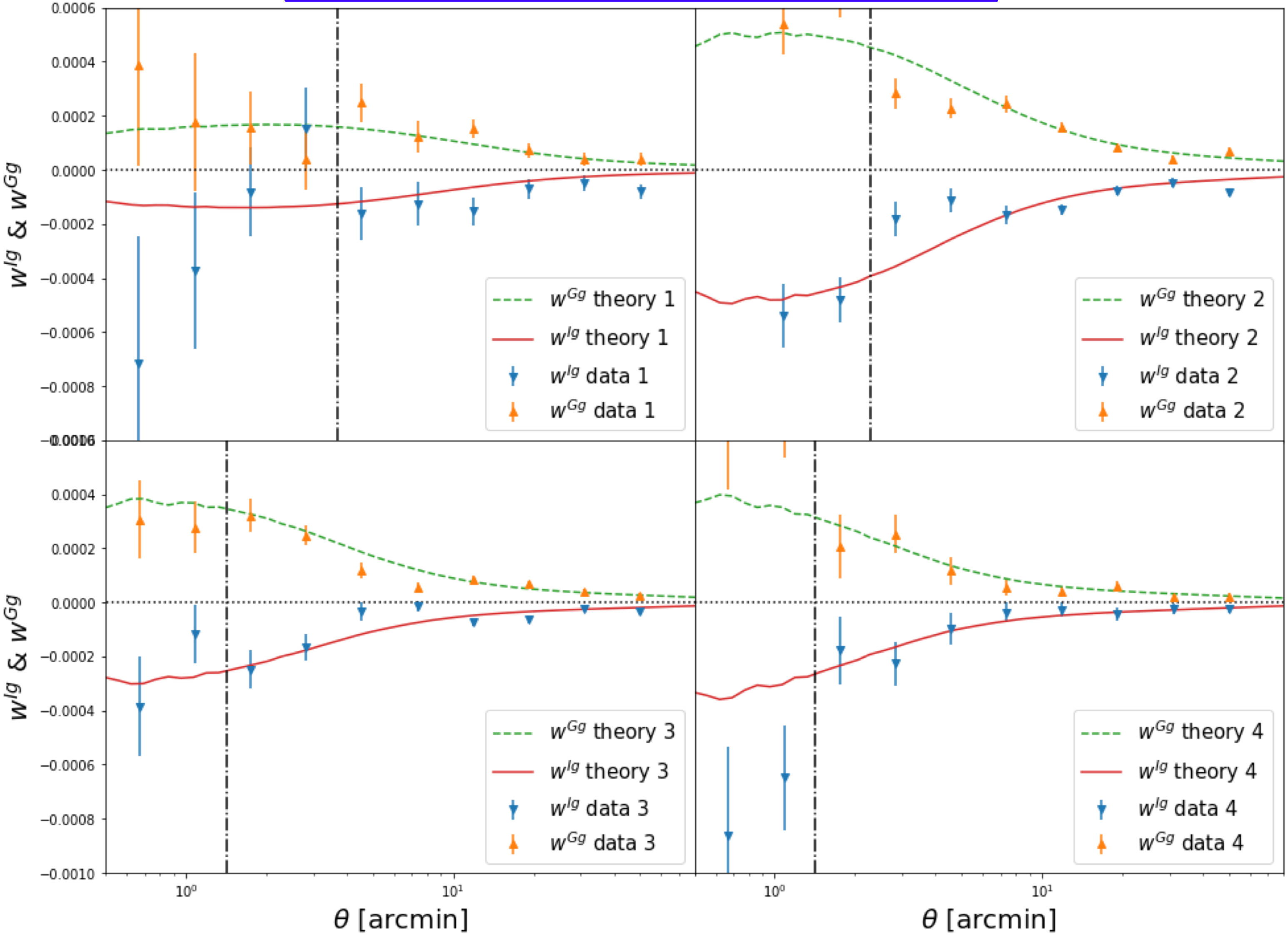

G

I

Application to DECaLS: blue galaxies

Null detection

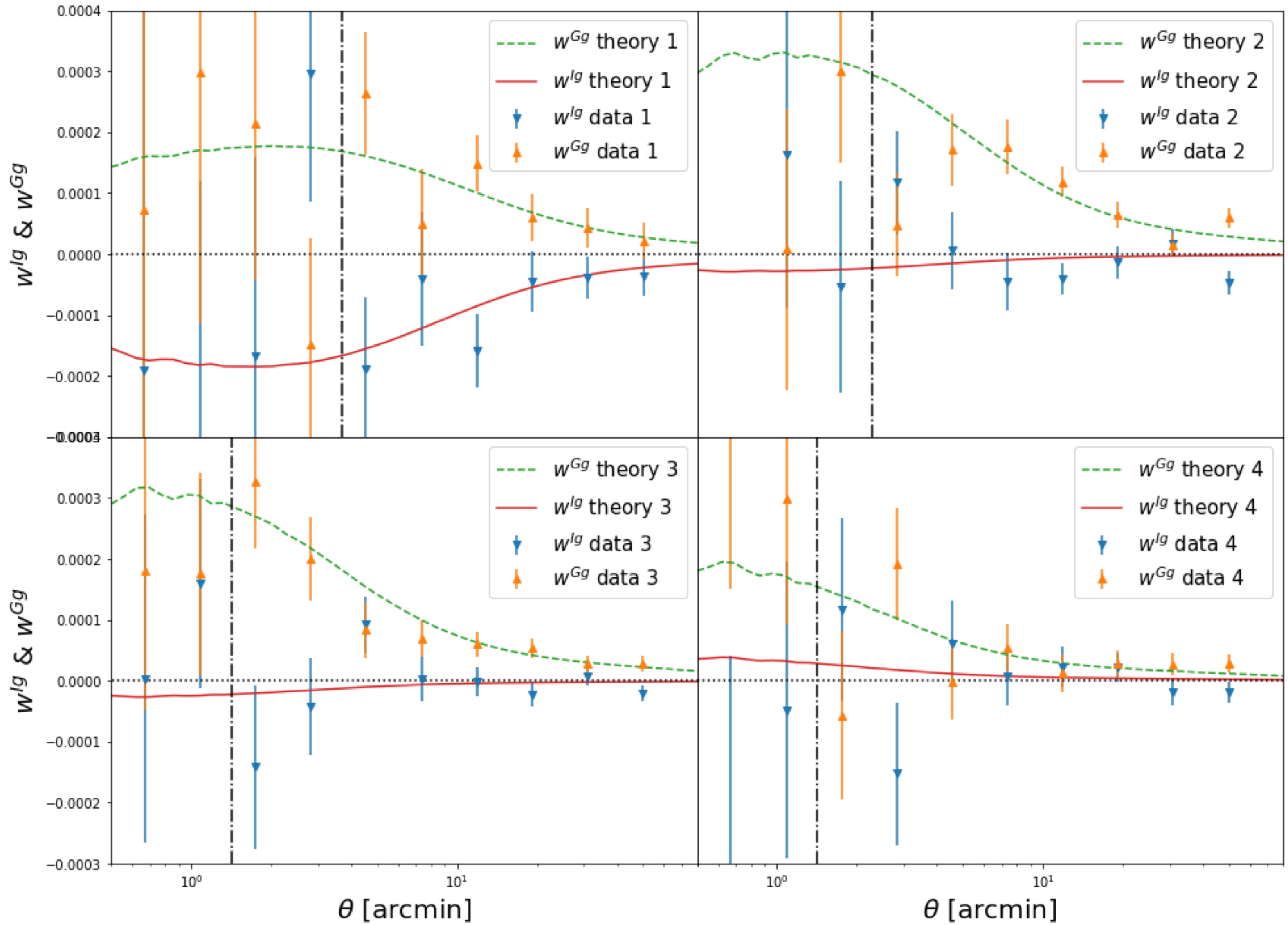

G
I

Application to DECaLS:

compare with the nonlinear tidal alignment model

$$P_{\delta,\gamma^I} = -A_{\mathrm{IA}}(L,z)\frac{C_1\rho_{m,0}}{D(z)}P_\delta(k;\chi)$$

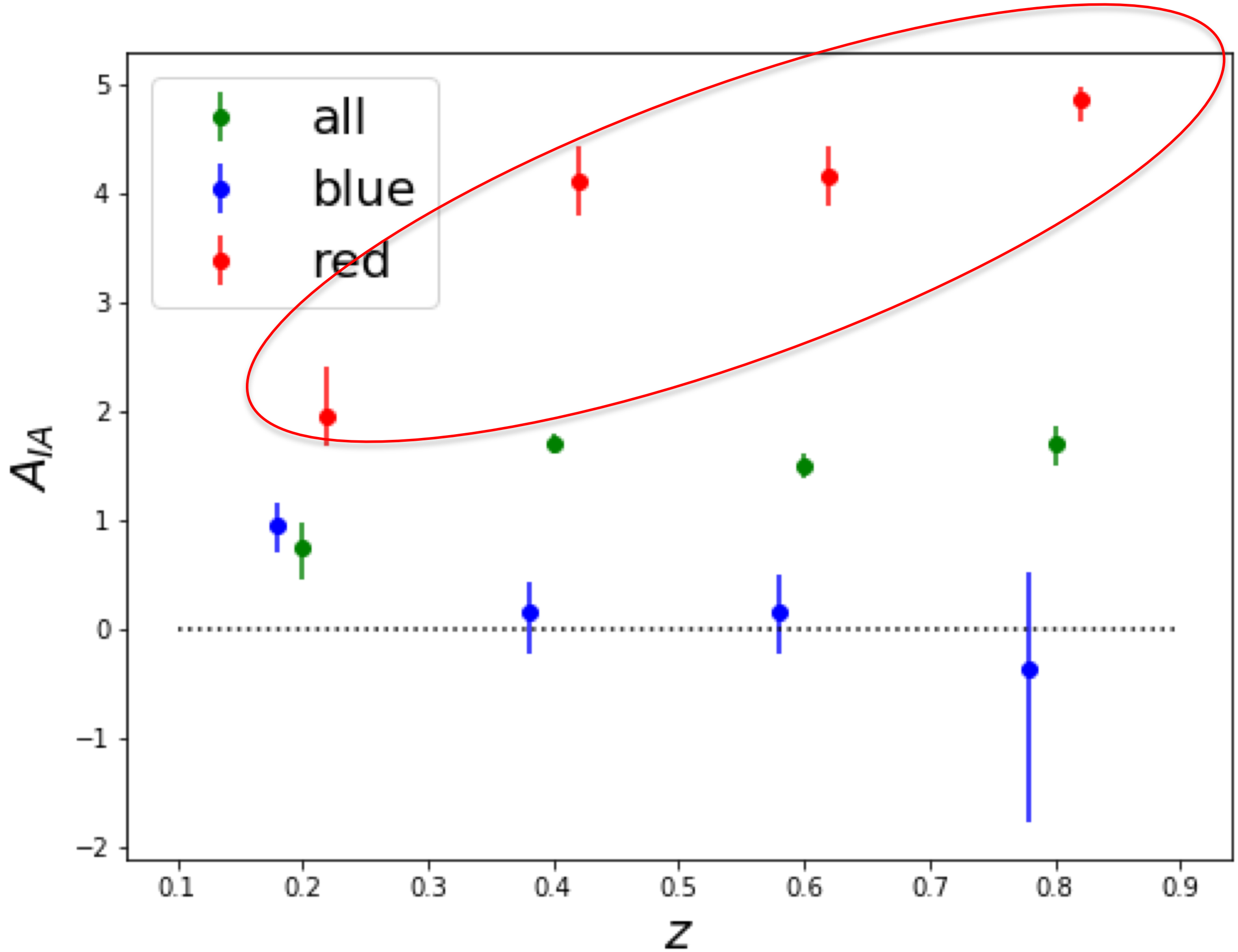

Caveats

- Photo-z
- Selection/mock
- Covariance matrix
- More robust tests/discriminations of IA models

- DR8
- Cosmic shear optimized surveys

Summary

- Weak lensing cosmology
- Systematic errors in weak lensing cosmology
  - The intrinsic alignment
  - Self-calibrating the intrinsic alignment
  - Detected IA in KiDS450/KV450 & DECaLS DR 3
  - Detected the redshift and color dependence

  - IA, an emerging tracer of LSS （stay tuned)